Accepted Manuscript

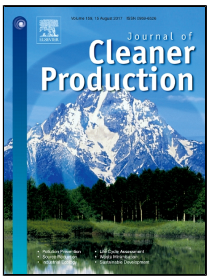

Utilization of fruit processing industry waste as green activated carbon for the treatment of heavy metals and chlorophenols contaminated water

Sabolč Pap, Tatjana Šolević Knudsen, Jelena Radonić, Snežana Maletić, Saša M. Igić, Maja Turk Sekulić

PII:	S0959-6526(17)31253-2
DOI:	10.1016/j.jclepro.2017.06.083
Reference:	JCLP 9833
To appear in:	*Journal of Cleaner Production*
Received Date:	03 February 2017
Revised Date:	02 June 2017
Accepted Date:	10 June 2017

Please cite this article as: Sabolč Pap, Tatjana Šolević Knudsen, Jelena Radonić, Snežana Maletić, Saša M. Igić, Maja Turk Sekulić, Utilization of fruit processing industry waste as green activated carbon for the treatment of heavy metals and chlorophenols contaminated water, *Journal of Cleaner Production* (2017), doi: 10.1016/j.jclepro.2017.06.083

Utilization of fruit processing industry waste as green activated carbon for the treatment of heavy metals and chlorophenols contaminated water

Sabolč Pap[a], Tatjana Šolević Knudsen[b], Jelena Radonić[a], Snežana Maletić[c], Saša M. Igić[d], Maja Turk Sekulić[a,*]

[a] *Faculty of Technical Sciences, Department of Environmental Engineering and Occupational Safety and Health, University of Novi Sad, Trg Dositeja Obradovića 6, 21 000 Novi Sad, Serbia*

[b] *Institute of Chemistry, Technology and Metallurgy, University of Belgrade, Njegoševa 12, 11 000 Belgrade, Serbia*

[c] *Faculty of Science, Department of Chemistry, Biochemistry and Environmental Protection, University of Novi Sad, Trg Dositeja Obradovića 3, 21 000 Novi Sad, Serbia*

[d] *Faculty for Economics and Engineering Management, University Business Academy in Novi Sad, Cvećarska 2, 21 000 Novi Sad, Serbia*

*Corresponding author. Tel.: +381 21 485-2498

E-mail address: majaturk@uns.ac.rs

Abstract

Plum stones, as a part of industrial and municipal organic waste, were used as a precursor for preparation of a low-cost activated carbon. Engineered, thermochemically-modified adsorbent was used to remove lead (Pb^{2+}), cadmium (Cd^{2+}), nickel (Ni^{2+}) and chlorophenols from an aqueous solution. The characterization of the medium was performed using standard instrumental analysis. Additionally, the assessment included the influence of pH, adsorbent dosage, temperature, contact time and initial metal concentration on the separation efficiency in the batch-operational mode. With optimal working conditions, the process efficiency of over 95% was accomplished. The equilibrium and kinetic studies of adsorption were done. The pseudo-second order model described the adsorption kinetics best. The maximum adsorption capacity of the engineered adsorbent for Pb^{2+}, Cd^{2+} and Ni^{2+} ions was calculated from the Langmuir isotherms and found to be 172.43 mg g^{-1}, 112.74 mg g^{-1} and 63.74 mg g^{-1}, respectively. Preliminary results indicate a strong affinity of the separation medium for chlorophenols. Thermodynamic parameters such as Gibbs energy, enthalpy and entropy were calculated. Regeneration of the saturated adsorbent was conducted, with diluted phosphoric acid produced as a waste stream, during the washing of the adsorbent after activation. Based on the desorption study results, the activated carbon was successfully regenerated in 3 cycles. Mutual influence of ions was analyzed in multicomponent systems. The real system production and operational costs analysis

confirmed a possibility for a successful implementation of the highly efficient, eco-friendly engineered adsorbent in the field of cost-effective wastewater treatment.

Keywords: Activated carbon, Green technology, Wastewater treatment, Heavy metal, Chlorophenol, Plum stone

1. Introduction

The increasing concentration of heavy metals in the water is mainly due to the wastewater discharges from industries. The methods that are most commonly used to remove metal ions and organic compounds from wastewaters are various conventional methods, such as chemical precipitation, filtration, flocculation, ion exchange, electrochemical treatments, etc. (Wang et al., 2015; Sadeek et al., 2015). The major disadvantages of these methods are their insufficient selectivity, production of waste sludge, which requires further treatments, high operating costs and various technical limitations, especially when the concentrations of the pollutants are low (Kang et al., 2016). In recent years, more and more attention is paid to non-conventional methods of wastewater treatment. This period of human history is considered the beginning of the development of adsorption with different lignocellulosic waste materials, or the application of biologic waste materials for the removal of pollutants from aqueous solutions (Lu and Gibb, 2008; Mouni et al., 2011). Attractiveness of this technique can be seen through the constant increase in the number of published scientific papers in this field, which only confirms the complexity and multidisciplinary nature of this approach (Gadd, 2009). Additionally, in the following years Serbia should solve Chapter 27 on the Environment (negotiating chapters of the European Union), and in that respect, low-cost green technologies for the treatment of wastewaters are of crucial importance.

Various plant materials, being easily accessible, economically and environmentally friendly, are gaining increasing importance as precursors for the production of cheaper activated carbon with specific structure and properties. Some of the plant materials that have been successfully used for this are: forest biowaste (Kim et al., 2015), pine cone (Özhan et al., 2014), blue jacaranda and plum stones (Trevino-Cordero et al., 2013), grape processing wastes (Saygılı et al., 2015), Brazilian pine-fruit shell (Royer et al., 2009), pistachio nut shells (Nowicki et al., 2015), cherry/sweet cherry kernels (Pap et al., 2016), apricot stones (Soleimani and Kaghazchi, 2008), hazelnut husks (Imamoglu and Tekir, 2008), oil palm shell (Tan et al., 2008), corncob (Sych et al., 2012), tomato processing solid waste (Saygılı and Güzel, 2016), coffee grounds (Reffas et al., 2010), wooden precursors (Largitte et al., 2016; Hajati et al., 2015), sea-buckthorn stones (Mohammadi et al., 2010).

The aim of the research presented in this paper was the selection, synthesis, characterization and efficiency evaluation of an alternative adsorption medium for the separation of inorganic ions and organic pollutants from model solutions and real wastewater samples. The main source of biomass used for production of activated carbon was lignocellulosic material (plum stone), as a waste byproduct of fruit processing industry. The activated carbon was prepared by thermochemical

conversion. In order to minimize the operating costs, which is one of the main challenges of most research studies, the preparation process of activated carbon was conducted in the complete absence of inert atmosphere. Carbonization was performed in a furnace exposed to air, without the application of any inert gases. The resulting activated carbon has been characterized by numerous instrumental analyses: elemental analysis, Fourier Transform Infrared Spectroscopy (FTIR), Scanning Electron Microscopy (SEM), Energy-dispersive X-ray spectroscopy (EDX) and Brunauer, Emmett and Teller (BET) technique. As a part of this study, the impact of the variability of different process parameters (pH value, the amount of adsorbent, contact time of the adsorbent with an aqueous solution, temperature and the initial concentration of adsorbate) on the separation efficiency of adsorbate from aqueous solutions in a batch mode has been examined. After determining the most important characteristics of the activated carbon and optimal process parameters, the kinetic, equilibrium and thermodynamic studies of adsorption on this separation medium were conducted in a batch mode. The mutual influence of ions has been analyzed in multicomponent systems. The affinity of the adsorbent towards chlorophenols has been examined as well. A detailed analysis of the production cost and the application of activated carbon, obtained in the analysis of real samples, showed the possibility of successful implementation of the media produced in the field of separation technology for wastewater treatment.

The purpose of this work was to evaluate the possibility of using fruit processing industry waste as renewable, low cost and sustainable adsorbent for the removal of heavy metals and chlorophenols from wastewaters. These results may provide a solution for cleansing and reuse of this type of waste, which can reduce its disposal cost, finally resulting in the protection of the environment from pollution by organic and inorganic pollutants.

2. Material and methods

When using green activated carbons, the preparation and implementation costs are as important as the properties of the obtained adsorbent. Therefore, the characteristics of activated carbon should be identified during the production process and optimum operation conditions should be determined carefully.

2.1 Sample preparation and analysis of inorganic and organic pollutants

The chemicals employed in the experiment, lead nitrate $Pb(NO_3)_2$, cadmium sulfate octahydrate $3CdSO_4 \cdot 8H_2O$, nickel nitrate hexahydrate $Ni(NO_3)_2 \cdot 6H_2O$, concentrated hydrochloric acid (HCl), ammonium hydroxide (NH_4OH), were all of analytical grade and supplied by Fisher Scientific. Stock solutions were prepared and diluted to the required concentrations using deionized water (EASYpure® II Reservoir Feed Water Purification System). The Pb^{2+}, Cd^{2+} and Ni^{2+} content in the supernatant was measured using flame atomic absorption spectrometry (FAAS, model Thermo Scientific S Series) with an air-acetylene flame.

The chlorophenols used in this research (2,4 – dichlorophenol, 2,4,6 – trichlorophenol, 2,3,4,6 – tetrachlorophenol and pentachlorophenol) and brominated

phenols surrogate standards (2,4-dibromophenol and 2,4,6-tribromophenol) were purchased from LGC Standards - Dr. Ehrenstorfer GmbH. After each experiment, chlorophenols and bromophenols were derivatized to acyl derivatives directly, in the water samples with acetic anhydride, under basic conditions. The investigated compounds were extracted using liquid-liquid extraction technique, with dichloromethane as solvent. The chlorophenols (in the form of acyl derivatives) were quantitatively analyzed against the internal surrogate standards, using gas chromatography–mass spectrometry (GC-MS, model Agilent 7890B, with HP5-MS capillary column, 30 m × 0.25 mm, film 0.25 μm).

2.2 Untreated lignocellulosic biomass

Plum (*Prunus domestica* L.) is a fruit tree from the plum family (*Prunoidae*), which is widespread in Serbia and belongs to the group of trees that are frequently found in orchards and tree-lined streets. The seeds of the fruit have no practical application and, when separated from the fleshy part, they must be collected and transported to a landfill site. Since the stones are rich in organic carbon, their use for production of powdered activated carbon is examined in this paper. The average production of plums in Serbia amounts up to 600 000 t y^{-1}. Stone weight is 20 % of the total weight of the fruit. Accordingly, it can be calculated that approximately 120 000 tons of this vegetable waste is produced annually. The basic characteristics and the appearance of this raw material after grinding are shown in Table 1 and Fig. 1.

2.3. Activated carbon preparation

Local plum stones were collected from a fruit plantation located in Novi Becej, province of Vojvodina (Serbia) and washed in water prior to peel separation. The plum stones (kernels and shells) were crushed in a mechanical mill and dried for 2 h at 105 ºC. The milled raw materials were impregnated with 50 wt.% H_3PO_4 aqueous solution at a ratio of 2.66:1 (weight). This corresponds to 1 kg of stones impregnated with 2 L of 50 vol.% acid. The mixture of the raw material and activating agent was allowed to stand for the next 24 h at room temperature (22.0 ± 1.0 ºC) and then the suspension was filtered to remove the residual acid. Subsequently, impregnated samples were placed in ceramic crucibles, air dried at room temperature for 2 h and then introduced into an electric furnace. During the first phase of carbonization the samples were heated at a rate of 10 ºC min^{-1} to 180 ºC and held at this temperature for 45 min in an air atmosphere at constant temperature. In the second phase, under identical atmosphere conditions, the samples were heated at a rate of 10 ºC min^{-1} to 500 ºC and held for the next 60 min. The product obtained was rinsed several times with distilled water until neutral pH values were reached, indicating that the phosphates and ash were eliminated, which helps opening and developing the porosity of the carbon. The pH was measured using a pH meter WTW SenTix® 41 (WTW, Germany). Finally, the material was dried in an oven at a temperature of 110 °C for at least 3 h. The particle size distribution of the activated carbon obtained was determined to be between 100 and 200 μm. Prepared activated carbon (Fig. 1) after

H_3PO_4 treatment and carbonization will be referred to as PPhA (**P**lum **Ph**osphoric **A**cid).

2.4. Characterization of the raw material and activated carbon

Elemental analysis (percentage content of carbon, hydrogen, nitrogen and sulfur in row kernels and PPhA) was performed by Vario EL III C, H, N, S/O Elemental Analyzer (Elementar, Germany). The oxygen contents were calculated based on difference.

The lignin, celluloses and proteins in raw lignocellulosic material were determined according to Klason, Kushner-Hoffer and Kjeldahl methods, respectively.

The moisture content was determined using American Standard Test Method (ASTM) D2867-04. Total ash content was determined by the ASTM D2866-94 method. The density of the sample was determined using graduated cylinder volume of 10 mL. All of the obtained results are shown in Table 1 and 2.

The yield of activated carbon, which is an indication of activation process mass efficiency, is the amount of activated carbon produced at the end of the activation step. The following equation is used to calculate the yield of activated carbon:

$$Yield(\%) = \frac{w_0 - w_c}{w_0} \times 100 \quad (1)$$

Where: w_o is the mass of material before carbonization and w_c is the mass of material after carbonization.

Suspension pH of the activated carbon in water (pH_{sus}) relates with the overall acidity of the adsorbent. The pH of water on initial contact with the activated carbon was determined according to the ASTM D6851-02 standard. The activated carbon sample (0.2 g) was suspended in 30 mL of distilled water and periodically stirred in a sealed plastic container for 72 hours. The pH value measured after this process was declared contact pH. The pH at the point zero charge (pH_{pzc}) was also determined. pH_{pzc} of activated carbon is important because it indicates the net surface charge. To determine the pH_{pzc}, 0.1 g of PPhA was transferred to nine 50 mL plastic bottles containing 30 mL of 0.1 mol L^{-1} KNO_3 with adjusted pH values from 2 to 10. The plastic vials were sealed and placed in a mechanical stirrer Heidolph Unimax 1010 (Heidolph, Germany) for 24 h. The content of the flasks was filtered and pH was measured. The pH value of the solution, which after contact with activated carbon remained unaltered, is considered to be pH_{pzc}.

The microstructures of the PPhA were determined using the SEM JSM 6460LV instrument (JEOL, USA), with an EDX attachment. PPhA BET surface area (S_{BET}) was determined by measuring N_2 adsorption, applying the BET method and an Autosorb iQ instrument (Quantachrome, USA). The cumulative pore volume for mesoporous was calculated using Barrete-Joynere-Halenda (BJH) method. The Dubinine-Radushkevich (DB) test was applied to get the micropore volume.

Chemical characterizations were studied by FTIR spectroscopy in order to identify the functional groups at the surface of the PPhA. FTIR spectra were recorded with a FTIR/NIR spectrophotometer Nexus 670 (Thermo Nicolet, USA), at wavenumbers from 400 to 4000 cm^{-1}.

2.5. Batch adsorption experiment

The effects of the experimental parameters such as pH (2.0 – 9.0), adsorbent dosage (0.2 – 10 g L^{-1}), contact time (5 – 60 min), temperature (295, 305 and 315 K) and the initial metal concentration (5 – 500 mg L^{-1}) on the adsorbate removal of metal ions were studied in a batch mode. pH was adjusted with 0.1 mol L^{-1} HCl or 0.1 mol L^{-1} NH_4OH. For all experimental studies, the exact quantity of PPhA was put in contact with 50 mL of metal solutions in Erlenmeyer flasks. The flasks were then placed on a rotary shaker at 140 rpm and the samples were taken at regular time intervals. The amount of pollutant adsorbed by activated carbon q_e (mg g^{-1}) is calculated by using the following equation:

$$q_e = \frac{(C_0 - C_e)}{m} \cdot V \quad (2)$$

Where C_0 is the initial adsorbate concentration and C_e is the residual adsorbate concentration (mg L^{-1}), V is the volume of solution (L) and m is the mass of the activated carbon (g).

The adsorbate removal percentage can be calculated as follows:

$$R\% = \frac{C_0 - C_e}{C_0} \cdot 100 \quad (3)$$

Furthermore, the root mean square error (*RMSE*) and sum of the squares of the errors (*ERRSQ*) tests were used to analyse the errors in experimental data, which can be described as:

$$RMSE = \sqrt{\frac{1}{N-2}\sum_{i=1}^{N}(q_e^{meas} - q_e^{cal})^2} \quad (4)$$

$$ERRSQ = \sum_{i=1}^{N}(q_e^{cal} - q_e^{meas})^2 \quad (5)$$

Where q_e^{meas} is the observation from the batch experiment, q_e^{cal} is calculated ion concentration with kinetic and isotherm models and N is the number of the samples. Smaller *RMSE* and *ERRSQ* mean that the equation can predict the experiment results more accurately (Rostamian et al., 2011).

2.6. Desorption and regeneration studies

When aiming at commercial applications of activated carbon and the prevention of potential contamination of the environment with contaminated adsorbents, the regeneration of PPhA is of great importance (Kołodyńska et al., 2011). The potential for PPhA reuse can be estimated on the basis of desorption degree of metal ions after the treatment and the efficiency of regenerated activated carbon. The PPhA sample

(3.0 g L^{-1}) was treated with a solution of Pb^{2+}, Cd^{2+} and Ni^{2+}, (total concentration of 300 mg L^{-1}), at the temperature 22.0 ± 1 °C, for 30 min. After the treatment, a desorption experiment was performed with diluted H_3PO_4. After washing and drying it, the activated carbon was reused as a regenerated adsorbent, in three repeated adsorption-desorption cycles. A diluted H_3PO_4 was produced as a waste stream during the washing of the activated carbon and after annealing at 500 °C. The experiments were conducted in a batch system. Desorption efficiency was calculated using the following equation:

$$d_E = \frac{q_d}{q_a} \times 100 \quad (6)$$

Where d_E is desorption efficiency (%), q_d is amount of metal ions desorbed (mg g^{-1}) and q_a is adsorption capacity of metal ions adsorbed on the activated carbon, (mg g^{-1}).

3. Results and discussion

In this section we investigated the properties of PPhA, the effect of operating conditions on the removal of heavy metals and chlorophenols, as well as conducted an analysis of production costs and costs of application of the obtained activated carbon.

3.1. Chemical and physical characteristics of the raw material

The elemental analysis results showed that the plum stones were mainly composed of carbon, oxygen and hydrogen (Table 1). The analyzed samples contain no sulfur. The nitrogen content is negligible, which is characteristic of lignocellulosic materials. Low content of nitrogen in the samples analyzed is a result of the low presence of nitrogen functional groups.

Table 1
Basic characteristics of the raw material

Raw material	Elemental analysis (%)					Cellulose (%)	Lignin (%)	Proteins (%)	Ash content (%)	Moisture content (%)	Density (kg m^{-3})
	C	O[a]	S	N	H						
Plum stones	45.6	46.5	n.d.[b]	0.3	6.7	22.9	25.4	3.0	0.8	2.3	550

[a]By difference

[b]Not detected

The analysis of the structural components showed that the material was composed mainly of cellulose and lignin (Table 1). The protein content is negligible. These are typical structural components of woody plant fruits and other similar fruits (seeds of other fruits, pumpkin, corn cobs, chestnuts, hazelnuts, peanuts etc.). The ash content is quite low (0.8 %). Bearing in mind that other similar materials have a much higher ash content, this is considered a good feature (Johnson et al., 2002). A moisture content of 2.3 % can be regarded as relatively low. In the case of solid, comminuted materials (such as fruit stones), a conclusion can be drawn about the internal structure of materials on the basis of the density, i.e. on its macro porosity and the manner in

which the particles are packaged in space. Density of plume stones used in this research is 550 kg m^{-3} which means that the raw material has a low density and great macroscopic porosity.

3.2. Characterization of activated carbon

The elemental analysis results showed that the activated carbon PPhA was mainly composed of carbon, oxygen and hydrogen (Table 2). Similar to the plum stone raw material, the activated carbon contains no sulfur, while the nitrogen content is negligible. However, if we take into account the content of carbon and oxygen, the difference in the elemental composition of the adsorbent before and after activation is significant. As a result of annealing the biomass at 500 °C, the content of carbon is increased, while the content of oxygen is reduced. Considering that activation, H_3PO_4 treatment and annealing, mainly result in hydrolysis of the functional groups, producing free functional groups of carboxylic acids and alcohols, the origin of reduced oxygen and increased carbon content is obvious. The proportion of mineral substances in PPhA was quite small (4.43 %) and, because of that, it was disregarded when determining the elemental composition.

Table 2
Chemical and physical characteristics of the PPhA

Activated carbon	Elemental analysis (%)					pH_{sus} (-)	pH_{pzc} (-)	Yield on 400 ºC (%)	Yield on 500 ºC (%)	Density (kg m^{-3})	Moisture content (%)	Ash content (%)
	C	O [a]	S	N	H							
PPhA	66.0	31.8	n.d.[b]	0.3	1.9	3.68	4.12	89.1	76.5	601	2.92	4.43

[a]By difference

[b]Not detected

Contact pH (pH_{sus}) is an indicator of overall predominance of acidic or basic functional groups on the surface of activated carbon. As the results in Table 2 show, PPhA leads to a significant decrease in the pH of distilled water. This feature classifies it as an L-type activated carbon that is hydrophilic, adsorbs basic compounds and lowers the pH of neutral solutions. The acidic nature of the final product is probably contributed to by the acidic agent, which was used during the activation process.

It is believed that the surface of each activated carbon, due to protonation of active centers, is positively charged at the pH values lower than pH_{pzc}. This should imply electrostatic repulsion of metal cations from the surface of the adsorbent. With a pH increase above pH_{pzc}, deprotonation of active sites or functional groups on the surface occurs, and the surface becomes more negative. As a result, the electrostatic repulsion of metal cations decreases, and their adsorption increases (Ghasemi et al., 2014b). The pH_{pzc} value for PPhA material is 4.12 (Table 2). When the pH is above this value, the functional groups have a more prominent negative charge and exhibit high affinity for oppositely charged ions, i.e. cations (Babic et al., 1999).

To ensure the complete transformation of organic compounds into graphene structures, carbonizing temperatures of 400 ºC and 500 ºC were used. The results in terms of the production yield of activated carbon, obtained at various activation temperatures are shown in Table 2. It should be emphasized that these activation results were achieved in the complete absence of an inert atmosphere, which essentially favors the development in the porosity of carbon. As Table 2 shows, the annealing temperature has strongly influences the yield. With an increase in the activation temperatures from 400 to 500 ºC, the production yield of activated carbon decreased from 89.1 to 76.5 % for PPhA. However, preliminary experimental findings indicate that the activation temperature of 500 ºC was highly effective in enhancing the activated carbon's adsorption capacity, which served as the fundamental basis for selecting the operating conditions for the further course of the study. Furthermore, subsequent rinsing and drying of the resulting product may lead to weight loss, and hence lower the final yield.

Based on the amount of generated waste materials and the yield of preparation process, approximate annual production of activated carbon was calculated. It was found that 91 800 t y^{-1} of activated carbon can be produced in Serbia from these type of waste materials.

Density is an important feature of powdered materials and provides information on its porosity and the manner in which the particles are packed in space. Thus, porous materials with a lower density have more air trapped in the structure. It was determined that PPhA activated carbon, synthesized in this research, has a density of 601 kg m^{-3} (see Table 2). The average apparent density of activated carbon ranges from 300 to 600 kg m^{-3}, which correlates with the obtained results.

For activated carbon samples, moisture and ash content are the important parameters that are directly related to the structure and reactivity of materials. Moisture adsorbed in the structure of activated carbon blocks the pores of the material, making them unavailable for the ions in the solution (Özer and Dursun, 2007). Ash in activated carbon is an impurity and an undesirable product, because it reduces the mechanical strength and porosity of activated carbon (Soleimani and Kaghazchi, 2007). The consequence of these effects is reflected in the reduction of the activated carbon adsorption capacity for ionic species in the solution. With a decrease in the moisture and ash content, adsorption characteristics of the medium improve. In the present study, we found that the ash and moisture content in PPhA were low (Table 2). This consistent with the adsorption efficiency of the activated carbon, as discussed further in the remainder of the paper.

In order to investigate the morphological characteristics of the surface, a SEM analysis of activated carbon PPhA was conducted. SEM micrographs of the PPhA surface, before and after the adsorption of metal ions, are shown in Fig. 2a and Fig. 2b. Fig. 2a shows that the PPhA surface is not smooth, but very irregular, forming a relief, and porous with numerous cavities and canals. These structural properties result in a larger specific surface area and porosity of the activated charcoal, which are the essential prerequisites for good adsorptive capacity of the separation medium. (Largitte et al., 2016; Zhu et al., 2016). This morphology, on the one hand, originates

from the preserved configuration and structure of the plume stone, and on the other hand, from thermochemical activation. Macro- and mesopores, cavities and channels have a chaotic, irregular structure and orientation, which also contributes to a higher adsorption ability of the material for the pollutants examined. The presence of macropores enables the transfer of the aqueous phase by convection into the interior of PPhA, which results in a more effective diffusion of metal ions and organic molecules.

Fig. 2b shows that the adsorption of Pb^{2+}, Cd^{2+} and Ni^{2+} from aqueous solutions by PPhA causes a series of morphological alterations of the surface which are reflected in the partial distortion of macro- and mesopores, channels and cavities. Pores become more deformed, and not so marked as they were before adsorption. At x10000 magnification, the metal complexes with ligands of the activated carbon can be observed on the surface of the PPhA (circled area in the Fig. 2b). The authors assume that metal binding to functional groups of the adsorbents active centers leads to the cleavage of intramolecular bonds, with consequent partial distortion of the surface morphology. EDX analysis showed that the surface of activated carbon was mainly composed of C and O, which is characteristic of lignocellulosic materials. Phosphorus on the surface originates from the impregnating agent used in the activation process.

EDX spectrum of PPhA after adsorption of Pb^{2+}, Cd^{2+} and Ni^{2+} (Fig. 2b) shows peaks corresponding to the adsorbed Pb^{2+}, Cd^{2+} and Ni^{2+} ions, which is direct evidence that the adsorption of the investigated ions actually occurred.

Table 3

Comparison of the textural properties of the synthesized activated carbon

Sample	Activation process (-)	S_{BET} (m^2 g^{-1})	Micropore volume (cm^3 g^{-1})	Mesopore volume (cm^3 g^{-1})	Total pore volume (cm^3 g^{-1})	Average pore radius (nm)	Max. adsoption capacity (mg g^{-1})	Reference
PPhA	Chemical (H_3PO_4, 500°C, 2h)	829	0.346	0.044	0.418	1.008	172.43 (Lead)	This work
Plum stones	Physical (steam, 750°C, 2h)	354	0.168	-	0.194	2.460	106.30 (Phenol)	Juang et al., 2000
Plum stones	Physical (steam, 900°C, 2h)	1162	0.378	-	0.536	2.63	257.80 (Phenol)	Wu et al., 1999
Plum stones	Chemical (NaOH, 780°C, 3h)	1478	-	-	0.815	2.2	259.00 (Phenol)	Tseng, 2007
Plum stones	Chemical (KOH, 800°C, 1.5h)	2174	1.05	-	1.09	2.05	46.00 (Nitrogen dioxide)	Nowicki et al., 2010
Plum stones	Chemical (H_3PO_4, 800°C, 4h)	329	0.135	0.025	0.155	-	11.45 (Lead)	Trevino-Cordero et al., 2013

The results of the analysis of textural properties of the resulting activated carbon are shown in Table 3. First of all, it can be observed that PPhA has a highly developed BET surface area, which is the basic characteristic of activated carbons. The BET surface area of PPhA was evaluated to be 829 m^2 g^{-1}. The material has well developed micro and mesopore structure. The BJH adsorption cumulative volume of pores for PPhA was 0.044 cm^3 g^{-1}. The total pore volume and micropore volume of PPhA were determined to be 0.418 cm^3 g^{-1} and 0.346 cm^3 g^{-1}, respectively. The pore dimensions

are extremely important parameters in the case of adsorption on porous adsorbents. As Table 3 shows, both micropore (< 2 nm) and mesopore (2 – 50 nm) structures are present in the PPhA, but the micropore volume occupies approximately 80 % of the total pore volume, which is much more than the mesopore volume. Smaller particle sizes of a porous carbon ensure a higher rate of diffusion and adsorption (Acharya et al., 2009).

Of course, the bonding mechanism is usually based on some kind of physicochemical interaction, such as dipole-dipole interactions, ion-dipole, weak hydrogen bonding, ionic attraction, ion exchange, etc. Therefore, it is crucial that the adsorbent, in addition to the adequate textural preconditions, meets the requirement of having a chemically reactive surface, rich in functional groups.

The FTIR spectrum of PPhA is shown in Fig. 3, before (a) and after adsorption (b). The spectrum shows characteristic peaks that correspond to functional groups typical of activated carbon. The broad absorption band maximizing at 3381 cm^{-1} originates from the O–H deformation vibrations of hydroxyl groups involved in hydrogen bond building. The presence of the peak located around 2920 cm^{-1} corresponds to C-H vibrations in methyl and methylene groups. Peaks at 1599 cm^{-1} and 481 cm^{-1} are attributed to the deformation vibrations of the C=O bond in ketones, aldehydes, lactones, and in the carboxyl functional group. We assume that, in this region of the spectrum, there is also a small overlap with the signal of the C=C bonds of the aromatic ring, which is normally located around 1580 cm^{-1}. A strong band near 1200 cm^{-1}, with a shoulder at about 1080 cm^{-1}, might originate from the functional groups of phosphorus, deriving from the use of H_3PO_4 as an activating agent. For this reason, the peak at 1168 cm^{-1} can be attributed to the deformation vibrations of the P=O bond, which are involved in the formation of hydrogen bonding, as well as stretching vibrations of the C-O bonds in the P-O-C bridge. The shoulder at 1068 cm^{-1} is attributed to the P-O-C bonds in the acidic phosphate esters, as well as the symmetric vibrations in the P-O-P chain (Momčilović et al., 2011). The band around 987 cm^{-1} shows the presence of aromatics, amines and hydrocarbons on the surface. These functional groups have a high affinity toward heavy metal ions. The FTIR spectrum of metal-adsorbed PPhA shows low transmittance intensity and the shifted peak locations at different frequencies due to Pb^{2+}, Cd^{2+} and Ni^{2+} adsorption (Rai et al., 2014).

3.3. Parameters influencing adsorption

In this part, we investigated the effect of different process parameters on the adsorption of metal ions onto PPhA.

3.3.1. Effect of solution pH on adsorption

The pH of a solution is one of the most important parameters which influence the effectiveness and nature of the adsorption process. The pH of a solution affects chemistry of heavy metals and organic molecules, as well as nature and activity of functional groups of the adsorption medium. The influence of pH on the PPhA adsorption capacity for Pb^{2+}, Cd^{2+} and Ni^{2+} ions was studied in the pH range from 2.0

to 9.0. The solutions of single heavy metal ions (100 mg L^{-1}) were in contact with the adsorbent (2.0 g L^{-1}) for 30 min at 22.0 ± 1 ° C. The assessment was conducted for pH values up to 9.0. Already in the pH range of 6.5-7.0, the transformation of metals into the form of insoluble hydroxides was observed. Accordingly, at pH values higher than 7.0, the decrease in concentration of ions in the solution cannot be attributed to the process of adsorption alone. The results are shown in Fig. 4, and it can clearly be seen that the adsorption of metal ions on PPhA is significantly pH dependent. Depending on the pH value, the adsorption capacity for lead ranges from 31.12 to 48.01 mg g^{-1}, for cadmium from 6.34 do 49.66 mg g^{-1} and for nickel from 6.62 do 43.50 mg g^{-1}. Generally, with an increase in the pH value, the adsorption capacity of Pb^{2+}, Cd^{2+} and Ni^{2+} ions increase as well. The adsorption capacities for lead and cadmium increase significantly up to the pH 6.0, and for nickel up to the pH 9.0. However, as explained earlier, due to the precipitation of hydroxides, the increase in the capacity at pH values higher than 6.0 cannot be attributed to the adsorption process only. For lead and cadmium, the adsorption capacity values change slightly at the pH values higher than 6.

The pH of the solution also affects the surface charge of the adsorbent. pH_{pzc} is in the middle of the working pH range, as a result of protonation/deprotonation of all functional groups. When the pH of the solution is above pH_{pzc}, the active centers/functional groups have a more pronounced negative charge and, accordingly, have a high affinity for the oppositely charged ions, i.e. cations (Wang et al., 2011). Since the pH_{pzc} value of the PPhA materials is 4.12, it can be concluded that, at higher pH values, the surface of activated carbon will be negatively charged. Consequently, metal cations which freely diffuse to the PPhA surface will be electrostatically attracted by its negatively charged surface.

Based on the results of the assessment of the effect of pH on adsorption of Pb^{2+}, Cd^{2+} i Ni^{2+}, a pH value of 6 was selected as optimal for further experiments.

3.3.2. Effect of activated carbon dosage

The effect of the adsorbent dose was investigated at the initial concentrations of the investigated metals of 100 mg L^{-1} at 22.0 ± 1 °C and the pH value of 6.0, varying the concentration of PPhA from 0.2 to 10.0 g L^{-1}. An increase in the concentrations of PPhA from 0.2 to 2.0 g L^{-1} resulted in a significant decrease of the adsorption capacity for Pb^{2+}, Cd^{2+} and Ni^{2+} ions (Fig. 5). Any further increase in the concentration of PPhA up to 10.0 g L^{-1} did not result in a noticeable decrease in the adsorption capacity, for any of the metals investigated. The results show that the adsorption capacity curves for all three metals exhibit the same trend - a sudden drop that occurs with the increase in the dosage of the activated carbon. The decrease in the adsorption capacity at a higher dosage of PPhA is attributed to the increase in BET surface area of the adsorbent, i.e. increase in the number of available adsorption sites to bind the ions whose concentration in the solution is constant. The negligible change in the adsorption capacities of PPhA above 2.0 g L^{-1} might be attributed to the presence of excess active sites on the PPhA surface, relative to the constant concentration of metal ions in solution (Ghasemi et al., 2014b; Ghasemi et al., 2014c).

The adsorption capacity and removal efficiency of metal ions do not increase at a higher dosage of activated carbon due to overlapping and aggregation, but also electrostatic rejection of the adsorbent particles, which results in a decrease of the effective PPhA surface area and the number of available active sites (Nadeem et al., 2016). Additionally, high dosage of the activated carbon also reduces the efficiency of suspension mixing, which further slows down the mass transport. For all the aforementioned reasons, PPhA concentration of 2.0 g L^{-1} was considered as the optimum dose and was used for further adsorption tests. All these observations are consistent with the literature related to the adsorption of metal ions by different activated carbons made from lignocellulosic materials.

3.3.3. Effect of contact time

The effect of contact time on the adsorption of Pb^{2+}, Cd^{2+} and Ni^{2+} from aqueous solutions by PPhA is presented in Fig. 6. Batch adsorption tests were done at various time intervals (5, 10, 15, 20, 30, 40, 50 and 60 min) with an initial concentration of 100 mg L^{-1} of metal ions solution at the optimal pH (6.0) and room temperature (22 ± 1 °C). The PPhA dose was 0.1 g (2.0 g L^{-1}) in 50 mL of the solution.

The results show that the activated carbon has a large adsorption capacity for the removal of the investigated metals in a relatively short period of time, which is consistent with other studies that have investigated the adsorption of ions on alternative adsorbents (Li et al., 2010; Ghasemi et al., 2014a; Coelho et al., 2014).

Based on these results it can be observed that the adsorption of metal ions occurs in two phases. The initial phase is fast due to the high concentration of free active sites on the PPhA surface, and due to the high initial concentration of metals. In the second phase, a reduction in the number of available PPhA active sites and the reduction in residual concentrations of the pollutants occur. These two phenomena significantly reduce the rate of adsorption. Additionally, there is a possibility of the occurrence of the electrostatic repulsion on the surface due to the high amount of bounded cations (Badmus et al., 2007; Plaza Cazón et al., 2013). During the first 5 minutes the highest increase in the adsorption capacity for Pb^{2+}, Cd^{2+}, and Ni^{2+} ions was achieved: 41.18, 37.84 and 18.01 mg g^{-1}, respectively. After 5 min, a slower phase began, and the equilibrium was established after 30 min when the capacity for Pb^{2+}, $Cd^{2+}$and Ni^{2+} was 45.39, 44.99 and 21.20 mg g^{-1}, respectively. The assessment of the effect of contact time on the adsorption efficiency showed that after 30 minutes there was no significant change in the adsorption rate. Accordingly, as the optimum contact time, a 30 min period was chosen.

3.3.4. Effect of initial adsorbate concentration

The initial concentration of metal ions represents a driving force for mass transfer between the fluid and solid phase (diffusion parameter), as well as for chemical bonding of ions to active centers (kinetic parameter). The influence of the initial concentration of metal ions was studied at the following concentrations: 5, 10, 20, 50, 100, 200, 300 and 500 mg L^{-1}, while keeping all other parameters at optimum values: 22.0 ± 1 ° C, pH of 6.0, activated carbon dose of 2.0 g L^{-1} and the contact time of 30

min. When the initial concentration of metals in the model solutions increases, the removal efficiency for all three metals decreases. The curves in Fig. 7 show that the removal efficiency is highest at the initial concentration of Pb^{2+}, Cd^{2+} and Ni^{2+} ions of 5 mg L^{-1}, and the lowest at the initial concentration of 500 mg L^{-1}. A comparison of the curves in Fig. 7 revealed that the degree of reduction in separation efficiency is almost the same for lead and cadmium. In the case of nickel, increase of the initial concentration leads to a higher decline in the efficiency level. Although with the increase in the concentration of metal ions in the solution the absolute quantity of removed metal ions increases, the rate of adsorption is reduced. Solutions that contain lower concentrations of Pb^{2+}, Cd^{2+} and Ni^{2+} ions are able to reach the equilibrium faster because the active centers are considerably more numerous than the ions present in solution. Increased initial concentration of metal ions leads to competitive adsorption at a constant number of available active sites (Li et al., 2010; Serrano-Gomez et al., 2015). Fig. 7 shows that the amount of Pb^{2+}, Cd^{2+} and Ni^{2+} ions adsorbed on PPhA increases with the initial concentration of metals. At the initial concentration of 500 mg L^{-1} the adsorption maximum is reached at 171.56, 111.78 and 62.19 mg g^{-1}, for Pb^{2+}, Cd^{2+} and Ni^{2+} ions, respectively.

3.4. Adsorption kinetics

To the results of the study of the adsorption kinetics of metal ions on PPhA, three theoretical linearized kinetic models were fitted: pseudo-first order, pseudo-second order and intra particle kinetic model.

The pseudo-first kinetic model is expressed by the following equation:

$$\log(q_e - q_t) = \log q_e - \left(\frac{K_1}{2.303}\right)t \quad (7)$$

where K_1 (1 min^{-1}) is the equilibrium rate constant of the pseudo-first order adsorption and it is determined from the plot of log $(q_e - q_t)$ as a function of t.

The pseudo-second-order kinetic model can be represented by the equation:

$$\frac{t}{q_t} = \frac{1}{K_2 q_e^2} + \frac{1}{q_e}t \quad (8)$$

where K_2 (g mg^{-1} min^{-1}) is the pseudo-second order rate constant and it is determined from the plot of t/q_t as a function of t.

Table 4

Kinetic parameters for the adsorption of Pb^{2+}, Cd^{2+} and Ni^{2+} onto PPhA

Metal ion			Pb^{2+}	Cd^{2+}	Ni^{2+}
$q_{e,exp}$ (mg g^{-1})			47.015	45.475	24.69
Pseudo-first order	$q_{e,cal}$	(mg g^{-1})	10.858	26.233	9.846
	K_1	(min^{-1})	-0.104	0.12	-0.04
		R^2	0.936	0.938	0.953
		RMSE	0.212	0.241	0.070
		ERRSQ	0.225	0.291	0.030
Pseudo-second order	$q_{e,cal}$	(mg g^{-1})	47.729	47.4	25.845

	K_2	(g mg^{-1} min^{-1})	0.024	0.009	0.008
		R^2	0.999	0.999	0.993
		RMSE	0.002	0.016	0.069
		ERRSQ	$3.5 \cdot 10^{-5}$	0.002	0.024
Intraparticle diffusion	K_i	(mg g^{-1} min$^{-1/2}$)	0.926	1.729	1.291
	C	(mg g^{-1})	40.656	33.363	14.326
		R^2	0.831	0.873	0.959
		RMSE	0.876	1.381	0.561
		ERRSQ	4.609	11.449	1.890

Weber–Morris kinetic model of intra particle diffusion is given by equation:

$$q_t = K_i t^{1/2} + C \quad (9)$$

where K_i (mg g^{-1} min$^{-1/2}$) is the intra particle diffusion rate constant and it is determined from the plot of qt as a function of $t^{1/2}$.

The three mentioned kinetics models (Figs. 8, 9 and 10) constants, correlation coefficients and error functions for adsorption of Pb^{2+}, Cd^{2+} and Ni^{2+} ions onto PPhA are presented in Table 4. We observed that the adsorption kinetics follow the pseudo-second order model better than the pseudo-first order and intraparticle diffusion models for all of the metal ions, based on the models higher correlation coefficient ($R^2 > 0.99$) and its lower *RMSE* and *ERRSQ* values. The correlation coefficients obtained by the pseudo-first order model have low values for all metals investigated ($R^2 < 0.960$). The calculated q_e values, obtained by pseudo-first order model, were not meaningful and they were very low in comparison with the experimental results. The correlation coefficients, determined from the plot of t/q_t as a function of t, in the pseudo-second order model, have high values ($R^2 = 0.99$) for all three investigated metals at the contact time of 60 min. The theoretical q_e values obtained by the pseudo-second order model are close to the experimental results, with a difference of only 0.3 to 0.4 % (Table 4). All these observations suggest that the adsorption of Pb^{2+}, Cd^{2+} and Ni^{2+} ions by PPhA occurs according to the mechanism of the second order reaction, that the metal cation bonding process is, to a large extent, kinetically controlled, and that it belongs to chemisorption processes. Fig. 10 shows that three levels of diffusion are important for the process of adsorption of Pb^{2+}, Cd^{2+} and Ni^{2+} ions: the movement of adsorbates through the diffusion boundary layer, intra particle diffusion and attainment of equilibrium. Since the diffusion model for each metal is presented on the same graph, it is difficult to perceive the multilinearity of the results. Large variations in the q_t value spread the graph on the y axis and it is hard to notice three steps occurred in the adsorption process. The first sharp section is the external adsorption or instantaneous adsorption stage. The second section is attributed to the gradual adsorption stage, where intraparticle diffusion is rate-controlled, and the third part is the equilibrium stage. Based on these results we concluded that the adsorption of metal ions by PPhA is a complex combination of surface chemisorption processes,

and that the most significant rate controlling steps are boundary-layer diffusion and intra particle diffusion (Bouhamed et al., 2012).

3.5. Adsorption isotherms

The adsorption of metal ions onto PPhA has been described by linearized adsorption isotherms in order to determine which theoretical model is applicable to the investigated system. The experimental results were fitted with the following theoretical models of isotherms: Langmuir, Freundlich and Dubinin–Radushkevich.
The linear form of Langmuir isotherm is represented by the equation:

$$\frac{C_e}{q_e} = \frac{1}{q_{max}K_L} + \frac{C_e}{q_{max}} \quad (10)$$

where C_e is the equilibrium concentration of adsorbate (mg L^{-1}), q_e is the adsorption capacity at equilibrium (mg g^{-1}), K_L is the Langmuir equilibrium constant (L mg^{-1}) and q_{max} is theoretical monolayer saturation capacity (mg g^{-1}).
Freundlich isotherm is an empirical model and it assumes the existence of heterogeneous adsorption centers on the surface of the adsorbent. The linear form of this isotherm is represented by the equation:

$$logq_e = logK_f + \frac{1}{n}logC_e \quad (11)$$

where K_f is Freundlich isotherm constant (L g^{-1}), and n is Freundlich exponent which serves to describe strength of adsorption. Typically, $1/n$ values range between 0 and 1, and if $1/n$ is closer to 0, the adsorption intensity is higher.

Table 5

Langmuir, Freundlich and Dubinin–Radushkevich isotherm constants for Pb^{2+}, Cd^{2+} and Ni^{2+}

Metal ion			Pb^{2+}	Cd^{2+}	Ni^{2+}
$q_{max,exp}$ (mg g^{-1})			171.56	111.78	62.19
Langmuir	q_{max}	(mg g^{-1})	172.43	112.74	63.724
	K_L	(L mg^{-1})	0.041	0.052	0.028
	R^2		0.874	0.973	0.919
	RMSE		0.134	0.156	0.669
	ERRSQ		0.108	0.146	2.686
Freundlich	K_f	(L mg^{-1})	9.879	8.293	6.619
	1/n		0.564	0.505	0.371
	R^2		0.989	0.959	0.955
	RMSE		0.074	0.134	0.116
	ERRSQ		0.033	0.109	0.081
Dubinin–Radushkevich	q_{DR}	(mg g^{-1})	46.202	38.109	29.156
	K_{DR}	(mol^2 J^{-2})	$9.081\ 10^{-8}$	$1.120\ 10^{-7}$	$1.207\ 10^{-7}$
	E_{DR}	(kJ mol^{-1})	1.805	1.781	1.614

	R^2	0.610	0.647	0.766
	RMSE	1.036	0.981	0.606
	ERRSQ	6.436	5.773	2.201

For a more precise determination of the mechanism and the nature of the adsorption process, the Dubinin–Radushkevich isotherm was also use to analyze the results. This model is given by the equation:

$$\ln q_e = \ln q_{DR} - K_{DR}\varepsilon^2 \quad (12)$$

where qe (mg g^{-1}) is adsorption capacity, q_{DR} (mg g^{-1}) is maximum adsorption capacity and K_{DR} (mol^2 J^{-2}) is the activity coefficient related to the mean free adsorption energy E (kJ mol^{-1}) according to the equation:

$$E = \frac{1}{\sqrt{-2K_{DR}}} \quad (13)$$

ε is the Polanyi potential, which is calculated from the equation:

$$\varepsilon = RTln\left(1 + \frac{1}{C_e}\right) \quad (14)$$

where R is the gas constant (8.314 J mol^{-1} K^{-1}), T - is the absolute temperature (K) and C_e is equilibrium concentration of adsorbate in the solution (mg L^{-1}).

Each one of the aforementioned models was presented graphically (Figs. 11, 12 and 13) and subsequently linearly fitted. Based on the correlation coefficients obtained (see Table 5), we conclude that the experimental results can be described well with Langmuir and Freundlich adsorption models (R^2 > 0.80). The Dubinin–Radushkevich isotherm has lower correlation coefficients for all three metal ions. The values of different errors of nonlinear method are listed in Table 5. The values of *RMSE* and *ERRSQ* for the Freundlich model for Pb^{2+}, Ni^{2+} and Cd^{2+} ions were the smallest among the three isotherms. According to the Langmuir's model, heavy metal ions adsorbed in an energetically homogeneous surface, in a monolayer, and without any interactions between the adsorbed ions. All active centers are energetically equivalent, the surface is energetically uniform, so the adsorbed ions do not interact with each other and the equilibrium is attained when a monolayer of the adsorbate ions saturates PPhA. According to the Langmuir's model, a significant adsorption capacity for Pb^{2+}, Cd^{2+} and Ni^{2+} ions was achieved: 172.43 mg g^{-1}, 112.74 mg g^{-1} and 63.74 mg g^{-1}, respectively. The Freundlich model is consistent with the adsorption on an energetically heterogeneous surface, where the adsorbed molecules interact with each other, which points to the physical adsorption. The correlation coefficients for the adsorption of metal ions are higher in the Freundlich's model, compared to the Langmuir's model. For this reason, the interpretation of the Freundlich's constants was accepted in this study: constant K_f, which is the adsorption capacity and the parameter n, which reflects the degree of deviation from the linearity of adsorption. If the value of n = 1, the adsorption follows a linear function; for values n < 1, the adsorption is unfavorable, and if n > 1, the adsorption is favored (Demirbas et al., 2009). In the present research, the obtained values for n are higher than one, and, accordingly, the

adsorption is favored and the adsorption affinity for binding of Pb^{2+}, Cd^{2+} and Ni^{2+} ions on PPhA is high.

The Dubinin–Radushkevich model can explain the nature of the adsorption process, i.e. whether it proceeds via chemisorption or physisorption. According to this model, when the value of E is higher than 8 kJ mol^{-1}, the adsorption process can be considered a chemisorption (Dubinin and Radushkevich, 1974). The values of E, which are shown in Table 5, are lower than 8 kJ mol^{-1}, leading to the conclusion that the investigated adsorption is physical in nature. However, in the case of the adsorption of Pb^{2+}, Cd^{2+} and Ni^{2+} ions on PPhA, a low correlation with the Dubinin–Radushkevich model was found (small R^2 and high *RMSE* and *ERRSQ*). Because of that, the application of this model to this research is limited.

3.6. Adsorption thermodynamics

The temperature influences the adsorption equilibrium and the molecules diffusion within the pores of the adsorbent materials (Cotoruelo et al., 2012).

Table 6

Thermodynamic parameters for adsorption of Pb^{2+}, Cd^{2+} and Ni^{2+} onto PPhA

Metal	T (K)	ΔH^o (kJ mol^{-1})	ΔS^o (J mol^{-1} K^{-1})	ΔG^o (kJ mol^{-1})
Pb^{2+}	295.15	20.49	139.78	-20.77
	305.15			-22.17
	315.15			-23.56
Cd^{2+}	295.15	92.78	386.50	-21.30
	305.15			-25.16
	315.15			-29.03
Ni^{2+}	295.15	-1.42	56.61	-18.12
	305.15			-18.69
	315.15			-19.23

The thermodynamic parameters, including enthalpy change (ΔH^o), entropy change (ΔS^o) and Gibbs free energy change (ΔG^o), can be calculated according to the following equations:

$$\Delta G^{\circ} = -RT ln \frac{q_e}{C_e} \quad (15)$$

$$lnK_L = -\frac{\Delta H^{\circ}}{RT} + \frac{\Delta S^{\circ}}{R} \quad (16)$$

$$\Delta G^{\circ} = \Delta H^{\circ} - T\Delta S^{\circ} \quad (17)$$

where q_e is the amount of ions adsorbed per unit mass of PPhA (mg g^{-1}), C_e is the equilibrium concentration (mg L^{-1}), T is the temperature (K) and R is the gas constant (8.314 J mol^{-1} K^{-1}) (Lin et al., 2011).

The data of lnK_L versus $1/T$ were plotted and shown in Fig. 14. There is a good linear relationship with the values and the correlation coefficients $R^2 > 0.95$. The observed thermodynamic values of ΔH^o, ΔS^o and ΔG^o were calculated and are given in Table 6. As Table 6 shows, the negative values of ΔG^o increase slowly with the increase of the

temperature for all metal ions, revealing that the adsorption process is spontaneous and thermodynamically favorable. The positive ΔS^o indicate that the adsorption process is entropy-driven rather than enthalpy-driven and the disorder is increased at the solid/liquid interface during the adsorption process (Uma et al., 2013). Furthermore, the positive value of ΔH^o for the Pb^{2+} and Cd^{2+} also confirms the endothermic nature of the adsorption on PPhA and increasing temperature favors the adsorption process. The negative enthalpy value of $\Delta H^o < 0$ kJ mol^{-1} for Ni^{2+} confirms that the adsorption is exothermic and the result obtained with Dubinin–Radushkevich isotherm that the adsorption of Ni^{2+} on PPhA is physical in nature. Significantly lower adsorption capacities for Ni^{2+} can be attributed to the fact that physisorption mainly takes place on the surface of the PPhA.

3.7. Adsorption mechanism

In the literature, different mechanisms for the adsorption of metal cations on activated carbons have been interpreted. These include surface adsorption, chemisorption, ion exchange and ion trapping inside the meso and micropores. To understand the adsorption mechanism one must consider two points: the activated carbon structure and surface properties; and the structure of the adsorbate (Chowdhury et al., 2010).
As the FTIR spectrum shows (Fig. 3), the surface of PPhA is rich in chemically reactive phosphoric and oxygen containing functional groups, which have a stronger preference to metal species (Pb^{2+}, Cd^{2+} and Ni^{2+}). Lignocellulose derivative phosphocarbonaceous esters and pyrophosphate species, chemically bonded to the PPhA, create a better adsorption structure with a lot of phosphate and polyphosphate bridges that provide for an increased crosslink of the carbons. Surface adsorption is another mechanism by which metal ions may be bound to the PPhA. This mechanism is a surface reaction where a positively charged metal ion is attracted to a negatively charged surface without the exchange of ions or electrons (Özacar et al., 2008). This proposition is supported by the fact that the observed adsorption was strongly pH-dependent. The pseudo-second order kinetic and Langmuir isotherm model exhibited excellent correlation with the experimental data. Both models assume that the PPhA surface, containing reactive functional groups, is homogenous and that the operating adsorption mechanism is chemisorption. It was also observed that the intraparticle diffusion was not the dominating mechanism, but the PPhA has well-developed micro- and mesopore-structure where a metal ion can be trapped and adsorbed. The results of our study support the conclusion that the adsorption mechanism for the metals involves the following steps: the diffusion through the boundary layer, the intraparticle diffusion of cations into the pores of the activated carbon and the adsorption of the metal ions on the interior surface of the adsorbent.

3.8. Comparison of mutual influence of metal ions on the adsorption efficiency in binary and ternary systems

The mutual influence of Pb^{2+}, Cd^{2+} and Ni^{2+} ions on the adsorption efficiency of PPhA was tested in binary and ternary solutions with the following composition: Pb-Cd, Pb-Ni, Cd-Ni and Pb-Cd-Ni. The treatments were conducted under the following

conditions: the initial concentration of each metal was 100 mg L^{-1} (total concentration of metals in the binary system was 200 mg L^{-1}, and in ternary system 300 mg L^{-1}), initial pH was 6.0, the temperature 22.0 ± 1 °C, the amount of the activated carbon 2.0 g L^{-1} and the duration of the treatment 30 min.

The results presented in Fig. 15 show that the adsorption capacity of PPhA for Pb^{2+}, Cd^{2+} and Ni^{2+} in the binary and ternary solutions is lower than in the systems where the individual metals are present. Inhibition of adsorption by other ions is the least noticeable for Pb^{2+} ions. If Cd^{2+} ions or Ni^{2+} ions, or their mixture is present in a solution with the Pb^{2+} ions, the adsorption efficiency of lead is reduced by several percents only. The negligible inhibitory effect of cadmium and nickel on the adsorption of lead can be explained by the larger atomic radius and higher electronegativity of Pb^{2+}. Due to these properties, Pb^{2+} ions are more effective in binding to the oxygen functional groups of the PPhA active centers

The removal efficiency of Cd^{2+} ions is reduced by approximately 1 % in the presence of Pb^{2+} ions and by approximately 10 % in the presence of Ni^{2+} ions.

In the binary system Ni^{2+} - Pb^{2+}, the presence of Pb^{2+} ions caused the reduction of Ni^{2+} adsorption efficiency by approximately 1 %. In the binary system Ni^{2+} - Cd^{2+}, the presence of cadmium lowered the adsorption efficiency of nickel by 6 %. Ni^{2+} ions showed the strongest inhibitory action on adsorption of other investigated metal ions.

3.9. Desorption and regeneration studies

Desorption experiments were carried out in order to examine the possibilities for the reuse of PPhA and for the recovery of the metals. As a desorption agent, a diluted H_3PO_4 was used. This H_3PO_4 was produced as a waste stream during the washing of the activated carbon, following annealing. The results in Fig. 16 show that after three adsorption-desorption cycles (C1, C2 and C3), the desorption efficiency is above 50 % for all of the investigated metals. The results point to the reversibility of the adsorption process. The adsorption efficiency for lead and nickel on the regenerated adsorbent changed slightly between three cycles. However, in the case of cadmium, a higher reduction in the adsorption efficiency was observed (Fig. 16). After three adsorption-desorption cycles, the total decrease in the adsorption capacity of PPhA for Pb^{2+}, Cd^{2+} and Ni^{2+} ions were 9 %, 40 % and 6 %, respectively.

From the resulting acidic solution, the investigated metals can be separated in pure form by electrolysis or, if the extraction of pure metals is not relevant, by chemical precipitation. Obviously PPhA has significant desorption and regeneration potential. Based on these characteristics, it can be classified as an economical and environmentally friendly separation medium for water purification.

3.10. Comparison with other activated carbons

The adsorption efficiency for Pb^{2+}, Cd^{2+} and Ni^{2+} ions from aquatic systems by different alternative activated carbons is the subject of numerous research studies. The comparison of published results and the results of the research presented here is shown in Table 7.

Table 7

Comparison of adsorption capacity of metal ions with other adsorbents

Pb^{2+}			Cd^{2+}			Ni^{2+}		
Activated carbon	q_{max} (mg g^{-1})	Ref.	Activated carbon	q_{max} (mg g^{-1})	Ref.	Activated carbon	q_{max} (mg g^{-1})	Ref.
Raw plum stones	9.93	Present study	Raw plum stones	12.45	Present study	Raw plum stones	5.63	Present study
Papaya peel	38.81	Abbaszadeh et al., 2016	Papaya wood	17.22	Asma et al., 2005	Apricot stone	27.21	Kobya et al., 2005
Cow bone	32.10	Cechinel et al., 2014	Pomelo peel	21.83	Saikaew and Kaewsarn, 2009	*Peganum harmala*-L	68.02	Ghasemi et al., 2014a
Tea waste	65.00	Amarasinghe and Williams, 2007	Grapefruit peel	42.09	Torab-Mostaedi et al., 2013	Grapefruit peel	46.13	Torab-Mostaedi et al., 2013
Apricot stone	22.85	Kobya et al., 2005	*S. platensis*	73.64	Celekli and Bozkurt, 2010	Pine bark	56.20	Argun et al., 2009
Cherry/sweet sherry kernels	180.26	Pap et al., 2016	Apricot stone	33.57	Kobya et al., 2005	PPhA	62.19	Present study
PPhA	171.56	Present study	PPhA	111.78	Present study	*S. platensis*	69.04	Celekli and Bozkurt, 2010
Neem leaf powder	300.00	Bhattacharyya and Sharma, 2004	Cherry/sweet cherry kernels	198.74	Pap et al., 2016	Cherry/sweet cherry kernels	77.71	Pap et al., 2016
Tamarind wood	43.85	Acharya et al., 2009	Nut shells	126.58	Tajar et al., 2009	Fireweed	10.12	Dwivedi et al., 2015
Van apple pulp	15.96	Depci et al., 2012	Bagasse	27.47	Mohan and Singh, 2002	Doum seed	13.51	El-Sadaawy and Abdelwahab, 2014

3.11. Cost estimation of PPhA

Successful commercial implementation of a technique for adsorbate removal of contaminants from aqueous waste effluents depends largely on four factors: the cost of raw materials, the cost of activated carbon production, activated carbon properties and reuse, ability to use in the treatment of real waste effluents.

In the present study, the plum stones were collected from a fruit plantation located in Novi Becej, province of Vojvodina (Serbia), and this biomass (waste byproducts of the fruit industry) in Serbia is available free of cost.

The cost involved in the production of activated carbon from plum stones has not been reported yet as per literature review. The production cost of adsorbent consists of various steps: collection of raw meterial, preparation of activated carbon and reusability. The cost estimation of preparing 1 kg of PPhA has been calculated in U.S. dollars (USD) as follows:

I Cost of raw material (CRM) = 0.0 USD, since the raw material is locally and abundantly available.

II Cost of transport (CT) = 0.0 USD, difficult to predict, but in the case of commercial production, a 10% surcharge should be added to the overall cost.

III Cost of cleaning raw material (CCRM) = 0.0007 USD, the raw material was washed with tap water obtained from a laboratory setup. The cost of water usage (the price of tap water per liter × water consumption for 1 kg) = 0.0007 × 1 = 0.0007 USD.

IV Cost of size reduction (CSR) = 0.02 USD, the stones were crushed in a mechanical mill. The electricity consumption for 1 kg × cost of 1 unit = 0.1 × 0.2 = 0.02 USD.

V Cost of drying raw material (DRM) = 0.0 USD, as the drying will be done in natural conditions in the case of commercial production.

VI Cost of impregnation (CI) = 0.5 USD. Price of 50 % H_3PO_4 about 700 USD per ton.

VII Cost of carbonization (CC) = CH = cost of heating = hours × units × per unit cost = 2 × 1.0 × 0.2 = 0.4 USD

VIII Cost of washing the activated carbon (CCRM) = (CH) + (CW) = 0.0214 USD. The activated carbon was washed with distilled water obtained from a laboratory setup. Where CH = cost of heating (electricity consumption for 2 L distillation unit × cost of 1 unit) = 0.1 × 0.2 = 0.02 USD. CW = cost of water usage (the price of tap water per liter × water consumption for 1 kg) = 0.0007 × 2 = 0.0014 USD.

IX Cost of drying the activated carbon (DAC) = hours × units × per unit cost = 2 × 0.2 × 0.2 = 0.08 USD.

Therefore, the overall cost for PPHA production = 1.02 USD.

Cost of transport = 0.1 USD

Overhead charge = 0.1 USD

Net cost of PPhA production = 1.22 USD per kg or 1220 USD per ton.

The cost estimation for commercial PPhA production suggests that activated carbon preparation from the plum stones is a cost effective process. The net cost for PPhA production is estimated to be only 1.22 USD per kg, which is cheap when compared to other activated carbon products derived from plant biomass (Maheshwari and Gupta, 2011; Banerjee et al., 2016). In order to assess the efficiency and suitability of PPhA to remove metals ions from a real system, an adsorption study with industrial wastewater samples after the secondary treatment in a batch mode has been conducted. The results showed that about 5.0 g of activated carbon was sufficient to treat a wastewater volume of 10 L containing around 4 mg L^{-1} metals (Cd^{2+}, Pb^{2+} and Ni^{2+}), i.e. that with 1 kg of PPhA, 2 tons of metal-contaminated water can be treated. Therefore, the present study confirmed that PPhA, as a cost-effective, eco-friendly and viable activated carbon, could justifiably be used for the treatment of wastewater containing lead, cadmium and nickel.

3.12. Preliminary results of the adsorption capacity of PPhA for chlorophenols

In order to estimate the affinity of PPhA for organic pollutants, the influence of the adsorbent dosage on the removal of chlorophenols from aqueous solutions has been investigated. Three different dosages of activated carbon were used: 2, 10 and 20 mg in 100 mL of a solution with an initial concentration of chlorophenols of 500 ng L^{-1} (concentration of each individual chlorophenol compound in the solution). The pH was adjusted to pH 6 using 0.1 mol L^{-1} solution of NH_4OH. The flasks were then placed on a rotary shaker and stirred for 1 h at 140 rpm. Finally, the suspensions were filtered and the filtrates were further treated according to the procedure for analysis of chlorinated phenols.

Fig. 17 shows that the increase in the adsorbent mass and the number of chlorine atoms lead to the increase in the efficiency of removal of chlorophenols. By using 20 mg of the adsorbent in model solutions, a removal efficiency of approximately 80 % for dichlorophenol and trichlorophenol, and over 90 % for tetrachlorophenol and pentachlorophenol can be achieved. This paper presents only preliminary results of this experiment.

4. Conclusion

Using plum stones as a raw material, an activated carbon, which has significant adsorption affinity for heavy metals and organic pollutants, can be synthesized. The following parameters: pH (2 – 9), adsorbent dosage (0.2 – 10 g L^{-1}), contact time (5 – 60 min), temperature (295, 305 and 315 K) and the initial metal concentration (5 – 500 mg L^{-1}) were studied in a batch mode. The analysis of adsorption isotherms showed good agreement for all three theoretical models used. The adsorption kinetics can be best described by a pseudo-second order theoretical model. Thermodynamic constants were also evaluated, using equilibrium constants changing with temperature. The negative values of ΔG^{o} suggested that the adsorption was spontaneous in nature. Adsorption of heavy metals is favored under neutral conditions, because there is no competitive effect of protons to bind to the same adsorption active sites. Regeneration of the saturated adsorbent was conducted in three cycles with diluted H_3PO_4 produced as a waste stream during washing of the adsorbent after activation. A high efficiency of over 90 % was achieved. The mutual influence of ions was analyzed in multicomponent systems. A thorough analysis of production costs and costs of application of the obtained activated carbon in the treatment of real samples has been performed. These results show the possibility of apllications in the field of wastewater treatment. There is significant potential for the use of plum stones as a cheap and easily available natural raw material for the production of green activated carbon.

Acknowledgments:

We thank the Ministry of Education, Science and Technological Development of the Republic of Serbia (Projects: III46007 and 176006) for supporting this research. This project was partially supported by TEMPUS project *NETREL* ("Network for

education and training for public environmental laboratories"; *project financed by:* European Union, Brussels, Belgium).

References

Abbaszadeh, S., Rafidah, W.A.S., Webb, C., Ghasemi, N., Muhamad, I.I., 2016. Treatment of lead-contaminated water using activated carbon adsorbent from locally available papaya peel biowaste. J. Clean. Prod. 118, 210-222.

Acharya, J., Sahu, J.N., Mohanty, C.R., Meikap, B.C., 2009. Removal of lead(II) from wastewater by activated carbon developed from Tamarind wood by zinc chloride activation. Chem. Eng. J. 149, 249-262.

Amarasinghe, B.M.W.P.K., Williams, R.A., 2007. Tea waste as a low cost adsorbent for the removal of Cu and Pb from wastewater. Chem. Eng. J. 132, 299-309.

Argun, E.M., Dursun, S., Karatas, M., 2009. Removal of Cd(II), Pb(II), Cu(II) and Ni(II) from water using modified pine bark. Desalination 249, 519–527.

Asma, S., Waheed, A.M., Muhammad, I., 2005. Removal and recovery of heavy metals from aqueous solution using papaya wood as a new adsorbent. Sep. Purif. Technol. 45, 25-31.

Babic, B.M., Milonjic, S.K., Polovina, M.J., Kaludierovic, B.V., 1999. Point of zero charge and intrinsic equilibrium constants of activated carbon cloth. Carbon 37 (3), 477-481.

Badmus, M.A.O., Audu, T.O.K., Anyata, B.U., 2007. Removal of lead ion from industrial wastewaters by activated carbon prepared from periwinkle shells. Turk. J. Eng. Environ. Sci. 31, 251-263.

Banerjee, S., Mukherjee, S., LaminKa-ot, A., Joshi, S.R., Mandal, T., Halder, G., 2016. Biosorptive uptake of Fe^{2+}, Cu^{2+} and As^{5+} by activated biochar derived from *Colocasia esculenta*: Isotherm, kinetics, thermodynamics, and cost estimation. J. Adv. Res. 7, 597–610.

Bhattacharyya, K.G., Sharma, A., 2004. Adsorption of Pb(II) from aqueous solution by *Azadirachta indica* (Neem) leaf powder. J. Hazard. Mater. 113, 97-109.

Bouhamed, F., Elouear, Z., Bouzid, J., 2012. Adsorptive removal of copper (II) from aqueous solutions on activated carbon prepared from Tunisian date stones: equilibrium, kinetics and thermodynamics. J. Taiwan Inst. Chem. E 43, 741–749.

Cechinel, M.A.P., Ulson de Souza, S.M.A.G.U., Ulson de Souza, A.A., 2014. Study of lead(II) adsorption onto activated carbon originated from cow bone. J. Clean. Prod. 65, 342-349.

Celekli, A., Bozkurt, H., 2011. Biosorption of cadmium and nickel ions using *Spirulina platensis*: kinetic and equilibrium studies. Desalination 275, 141-147.

Chowdhury, S., Mishra, R., Saha, P., Kushwaha, P., 2010. Adsorption thermodynamics, kinetics and isosteric heat of adsorption of Malachite Green onto chemically modified rice husk. Desalination 265, 159–168.

Coelho, G.F., Gonçalves, Jr., A.C., Tarley, C.R.T., Casarin, J., Nacke, H., Francziskowski, M.A., 2014. Removal of metal ions Cd (II), Pb (II), and Cr (III) from water by the cashew nut shell *Anacardium occidentale L*. Ecol. Eng. 73, 514-525.

Cotoruelo, L.M., Marqués, M.D., Díaz, F.J., Rodríguez-Mirasol, J., Rodríguez, J.J., Cordero, T., 2012. Adsorbent ability of lignin-based activated carbons for the removal of p-nitrophenol from aqueous solutions. Chem. Eng. J. 184, 176-183.

Demirbas, E., Dizge, N., Sulak, M.T., Kobya, M., 2009. Adsorption kinetics and equilibrium of copper from aqueous solutions using hazelnut shell activated carbon. Chem. Eng. J. 148, 480–487.

Depci, T., Kul, A.R., Önal, Y., 2012. Competitive adsorption of lead and zinc from aqueous solution on activated carbon prepared from Van apple pulp: study in single- and multi-solute systems. Chem. Eng. J. 200–202 (34), 224–236.

Dubinin, M.M., Radushkevich, L.V., 1974. Equation of the characteristic curve of activated charcoal. Proc. Acad. Sci. USSR Phys. Chem. 55, 331–333.

Dwivedi, A.D., Dubey, S.P., Sillanpaea, M., Kwon, Y.-N., Lee, C., 2015. Distinct adsorption enhancement of bicomponent metals (cobalt and nickel) by Fireweed-derived carbon compared to activated carbon: incorporation of surface group distributions for increased efficiency. Chem. Eng. J. 281, 713-723.

El-Sadaawy, M., Abdelwahab, O., 2014. Adsorptive removal of nickel from aqueous solutions by activated carbons from doum seed (*Hyphaenethebaica*) coat. Alexandria. Eng. J. 53 (2), 399–408.

Gadd, G.M., 2009. Biosorption: Critical review of scientific rationale, environmental importance and significance for pollution treatment. J. Chem. Technol. Biotechnol. 84, 13–28.

Ghasemi, M., Ghasemi, N., Zahedi, G., Alwi, S.R.W., Goodarzi, M., Javadian, H., 2014a. Kinetic and equilibrium study of Ni(II) sorption from aqueous solutions onto *Peganum harmala*-L. Int. J. Environ. Sci. Technol. 11, 1835-1844.

Ghasemi, M., Naushad, M., Ghasemi, N., Khosravi-fard, Y., 2014b. A novel agricultural waste based adsorbent for the removal of Pb(II) from aqueous solution: kinetics, equilibrium and thermodynamic studies. J. Ind. Eng. Chem. 20, 454-461.

Ghasemi, M., Naushad, M., Ghasemi, N., Khosravi-fard, Y., 2014c. Adsorption of Pb(II) from aqueous solution using new adsorbents prepared from agricultural waste: adsorption isotherm and kinetic studies. J. Ind. Eng. Chem. 20, 2193-2199.

Hajati, S., Ghaedi, M., Yaghoubi, S., 2015. Local, cheap and nontoxic activated carbon as efficient adsorbent for the simultaneous removal of cadmium ions

and malachite green: Optimization by surface response methodology. J. Ind. Eng. Chem. 21, 760–767.

Imamoglu, M., Tekir, O., 2008. Removal of copper (II) and lead (II) ions from aqueous solutions by adsorption on activated carbon from a new precursor hazelnut husks. Desalination 228, 108-113.

Johnson, P.D., Watson, M.A., Brown, J., Jefcoat, I.A., 2002. Peanut hull pellets as a single use sorbent for the capture of Cu(II) from wastewater. Waste. Manage. 22, 471–480.

Juang, R., Wu, F., Tseng, R., 2000. Mechanism of adsorption of dyes and phenols from water using activated carbons prepared from plum kernels. J. Colloid. Interface. Sci. 227, 437–44.

Kang, Y., Gu, Z., Zhang, J., Xie, H., Liu, H., Zhang, C., 2016. Enhancement of Ni(II) removal by urea-modified activated carbon derived from *Pennisetum alopecuroides* with phosphoric acid activation. J. Taiwan. Inst. Chem. E. 60, 335–341.

Kim, N., Park, M., Park, D., 2015. A new efficient forest biowaste as biosorbent for removal of cationic heavy metals. Bioresour. Technol. 175, 629–632.

Kobya, M., Demirbas, E., Senturka, E., Ince, M., 2005. Adsorption of heavy metal ions from aqueous solutions by activated carbon prepared from apricot stone. Bioresour. Technol. 96, 1518–21.

Kołodyńska, D., Krukowska, J., Thomas, P., 2016. Comparison of sorption and desorption studies of heavy metal ions from biochar and commercial active carbon. Chem. Eng. J. 307, 353-363.

Largitte, L., Brudey, T., Tant, T., Couespel Dumesnil, P., Lodewyckx, P., 2016. Comparison of the adsorption of lead by activated carbons from three lignocellulosic precursors. Microporous. Mesoporous. Mater. 219, 265-275.

Li, Y., Du, Q., Wang, X., Zhang, P., Wang, D., Wang, Z., Xia, Y., 2010. Removal of lead from aqueous solution by activated carbon prepared from *Enteromorpha prolifera* by zinc chloride activation. J. Hazard. Mater. 183, 583-589.

Lin, J., Zhan, Y., Zhu, Z., 2011. Adsorption characteristics of copper (II) ions from aqueous solution onto humic acid-immobilized surfactant-modified zeolite. Colloid. Surface. A. 384 (1-3), 9-16.

Lu, S., Gibb, S.W., 2008. Copper removal from wastewater using spent-grain as biosorbent. Bioresour. Technol. 99, 1509–1517.

Maheshwari, U., Gupta, S., 2011. Kinetic and equilibrium studies of Cr (VI) removal from aqueous solutions using activated neem bark. Res. J. Chem. Environ. 15, 939–43.

Mohammadi, S. Z.M., Karimi, A., Afzali, D., Mansouri, F., 2010. Removal of Pb(II) from aqueous solutions using activated carbon from Sea-buckthorn stones by chemical activation. Desalination 262, 86-93.

Mohan, D., Singh, K.P., 2002. Single and multi-component adsorption of cadmium and zinc using activated carbon derived from bagasse – an agricultural waste. Water Res. 36, 2304–2318.

Momčilović, M., Purenović, M., Bojić, A., Zarubica, A., Ranđelović, M., 2011. Removal of lead (II) ions from aqueous solutions by adsorption onto pine cone activated carbon. Desalination 276, 53-59.

Mouni, L., Merabet, D., Bouzaza, A., Belkhiri, L., 2011. Adsorption of Pb^{2+} from aqueous solutions using activated carbon developed from Apricot stone. Desalination 276, 148-153.

Nadeem, R., Manzoor, Q., Iqbal, M., Nisar, J., 2016. Adsorption of Pb(II) onto immobilized and native *Mangifera indica* waste biomass. J. Ind. Eng. Chem. 35, 185-194.

Nowicki, P., Bazan, A., Kazmierczak-Razna, J., Pietrzak, R., 2015. Sorption properties of carbonaceous adsorbents obtained by pyrolysis and activation of pistachio nut shells. Adsorpt. Sci. Technol. 33, 581-586.

Nowicki, P., Wachowska, H., Pietrzak, R., 2010a. Active carbons prepared by chemical activation of plum stones and their application in removal of NO_2. J. Hazard. Mater. 181, 1088–1094.

Özacar, M., Sengil, I.A., Türkmenler, H., 2008. Equilibrium and kinetic data, and adsorption mechanism for adsorption of lead onto valonia tannin resin. Chem. Eng. J. 143 (1–3), 32–42.

Özer, A., Dursun, G., 2007. Removal of methylene blue from aqueous solution by dehydrated wheat bran carbon. J. Hazard. Mater. 146, 262-269.

Özhan, A., Sahin, O., Küçük, M.M., Saka, C., 2014. Preparation and characterization of activated carbon from pine cone by microwave-induced $ZnCl_2$ activation and its effects on the adsorption of methylene blue. Cellulose 21, 2457-2467.

Pap, S., Radonic, J., Trifunovic, S., Adamovic, D., Mihajlovic, I., Vojinovic Miloradov, M., Turk Sekulic, M., 2016. Evaluation of the adsorption potential of eco-friendly activated carbon prepared from cherry kernels for the removal of Pb^{2+}, Cd^{2+} and Ni^{2+} from aqueous wastes. J. Environ. Manage. 184, 297-306.

Plaza Cazón, J., Viera, M., Donati, E., Guibal, E., 2013. Zinc and cadmium removal by biosorption on *Undaria pinnatifida* in batch and continuous processes. J. Environ. Manage. 129, 423-434.

Rai, M.K., Shahi, G., Meena, V., Meena, R., Chakraborty, S., Singh, R.S., Rai, B.N. 2016. Removal of hexavalent chromium Cr (VI) using activated carbon prepared from mango kernel activated with H3PO4. Resours. Effici. Technolog. 2, 63–70.

Reffas, A., Bernardet, V., David, B., Reinert, L., Lehocine, M.B., Dubois, M., Batisse, N., Duclaux, L., 2010. Carbons prepared from coffee grounds by H_3PO_4 activation: characterization and adsorption of methylene blue and Nylosan Red N-2RBL. J. Hazard. Mater. 175, 779-788.

Rostamian, R., Najafi, M., Rafati, A.A., 2011. Synthesis and characterization of thiol-functionalized silica nano hollow sphere as a novel adsorbent for removal of poisonous heavy metal ions from water: kinetics, isotherms and error analysis. Chem. Eng. J. 171, 1004-1011.

Royer, B., Cardoso, N.F., Lima, E.C., Vaghetti, J.C., Simon, N.M., Calvete, T., Veses, R.C., 2009. Applications of Brazilian pine-fruit shell in natural and carbonized forms as adsorbents to removal of methylene blue from aqueous solutions: Kinetic and equilibrium study. J. Hazard. Mater. 164, 1213-1222.

Sadeek, S.A., Negm, N.A., Hefni, H.H.H., Abdel Wahab, M.M., 2015. Metal adsorption by agricultural adsorbents: Adsorption isotherm, kinetic and adsorbents chemical structures. Int. J. Biol. Macromol. 81, 400–409.

Saikaew, W., Kaewsarn, P., 2009. Peel pomelo: agricultural waste for adsorption of cadmium ions from aqueous solutions. World Acad. Sci. Eng. Technol. 56, 287-291.

Saygılı, H., Güzel, F., 2016. High surface area mesoporous activated carbon from tomato processing solid waste by zinc chloride activation: process optimization, characterization and dyes adsorption. J. Clean. Prod. 113, 995-1004.

Saygılı, H., Güzel, F., Onal, Y., 2015. Conversion of grape industrial processing waste to activated carbon sorbent and its performance in cationic and anionic dyes adsorption. J. Clean. Prod. 93, 84-93.

Serrano-Gomez, J., Lopez-Gonzalez, H., Olguín, M.T., Bulbulian, S., 2015. Carbonaceous material obtained from exhausted coffee by an aqueous solution combustion process and used for cobalt (II) and cadmium (II) sorption. J. Environ. Manage. 156, 121-127.

Soleimani, M., Kaghazchi, T., 2007. Agricultural waste conversion to activated carbon by chemical activation with phosphoric acid. Chem. Eng. Technol. 30, 649- 654.

Soleimani, M., Kaghazchi, T., 2008. Adsorption of gold ions from industrial wastewater using activated carbon derived from hard shell of apricot stones-an agricultural waste. Biores. Technol. 99, 5374–5383.

Sych, N., Trofymenko, S., Poddubnaya, O., Tsyba, M., Sapsay, V., Klymchuk, D., Puziy, A., 2012. Porous structure and surface chemistry of phosphoric acid activated carbon from corncob. Appl. Surf. Sci. 261, 75-82.

Tajar, F.A., Kaghazchi, T., Soleimani, M., 2009. Adsorption of cadmium from aqueous solutions on sulfurized activated carbon prepared from nut shells. J. Hazard. Mater. 165 (1–3), 1159–1164.

Tan, I., Ahmad, A., Hameed, B., 2008. Adsorption of basic dye using activated carbon prepared from oil palm shell: batch and fixed bed studies. Desalination 225, 13-28.

Torab-Mostaedi, M., Asadollahzadeh, M., Hemmati, A., Khosravi, A., 2013. Equilibrium, kinetic, and thermodynamic studies for adsorption of cadmium and nickel on grapefruit peel. J. Taiwan Inst. Chem. Eng. 44, 295-302.

Trevino-Cordero, H., Juarez-Aguilar, L.G., Mendoza-Castillo, D.I., Hernandez Montoya, V., Bonilla-Petriciolet, A., Montes-Moran, M.A., 2013. Synthesis and adsorption properties of activated carbons from biomass of *Prunus domestica* and *Jacaranda mimosifolia* for the removal of heavy metals and dyes from water. Ind. Crop. Prod. 42, 315-323.

Tseng, R.L., 2007. Physical and chemical properties and adsorption type of activated carbon prepared from plum kernels by NaOH activation. J. Hazard. Mater. 147 (3), 1020-1027.

Uma, Banerjee, S., Sharma, Y.C., 2013. Equilibrium and kinetic studies for removal of malachite green from aqueous solution by a low cost activated carbon. J. Ind. Eng. Chem. 19, 1099–1105.

Wang, H., Gao, B., Wang, S., Fang, J., Xue, Y., Yang. K., 2015. Removal of Pb(II), Cu(II), and Cd(II) from aqueous solutions by biochar derived from $KMnO_4$ treated hickory wood. Bioresour. Technol. 197, 356–362.

Wang, Z., Nie, E., Li, J., Zhao, Y., Luo, X., Zheng, Z., 2011. Carbons prepared from *Spartina alterniflora* and its anaerobically digested residue by H_3PO_4 activation: characterization and adsorption of cadmium from aqueous solutions. J. Hazard. Mater. 188, 29-36.

Wu, F.C., Tseng, R.L., Juang, R.S., 1999. Pore structure and adsorption performance of the activated carbons prepared from plum kernels. J. Hazard. Mater. 69, 287– 302

Zhu, G.Z., Deng, X., Hou, M., Sun, K., Zhang, Y., Li, P., Liang, F., 2016. Comparative study on characterization and adsorption properties of activated carbons by phosphoric acid activation from corncob and its acid and alkaline hydrolysis residues. Fuel Process. Technol. 144, 255–261.

LIST OF FIGURE CAPTIONS

Journal of Cleaner Production
Highlights

- ✓ Heavy metals and chlorophenols removal on green-activated carbon were studied.
- ✓ High specific surface area (879 m^2 g^{-1}) activated carbon was prepared.
- ✓ The adsorption capacity with 172.43 mg g^{-1} mainly depends on the surface chemistry.
- ✓ A novel activated carbon could be applied into wastewater treatment.
- ✓ Our approach is simple and inexpensive with the production cycle without any waste.

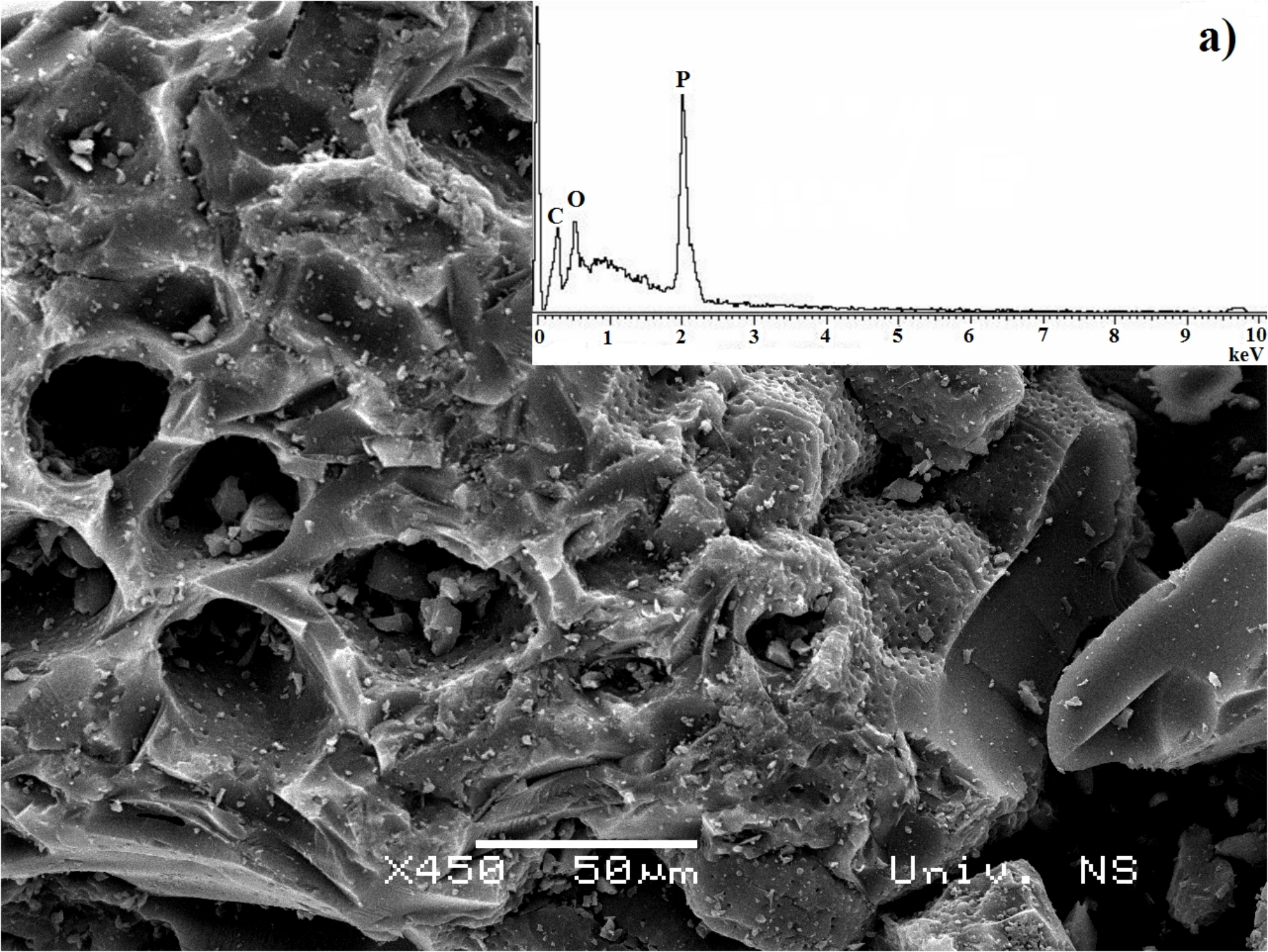
a)
P
C
O
0
1
2
3
4
5
6
7
8
9
10
keV
X450 50µm Univ. NS

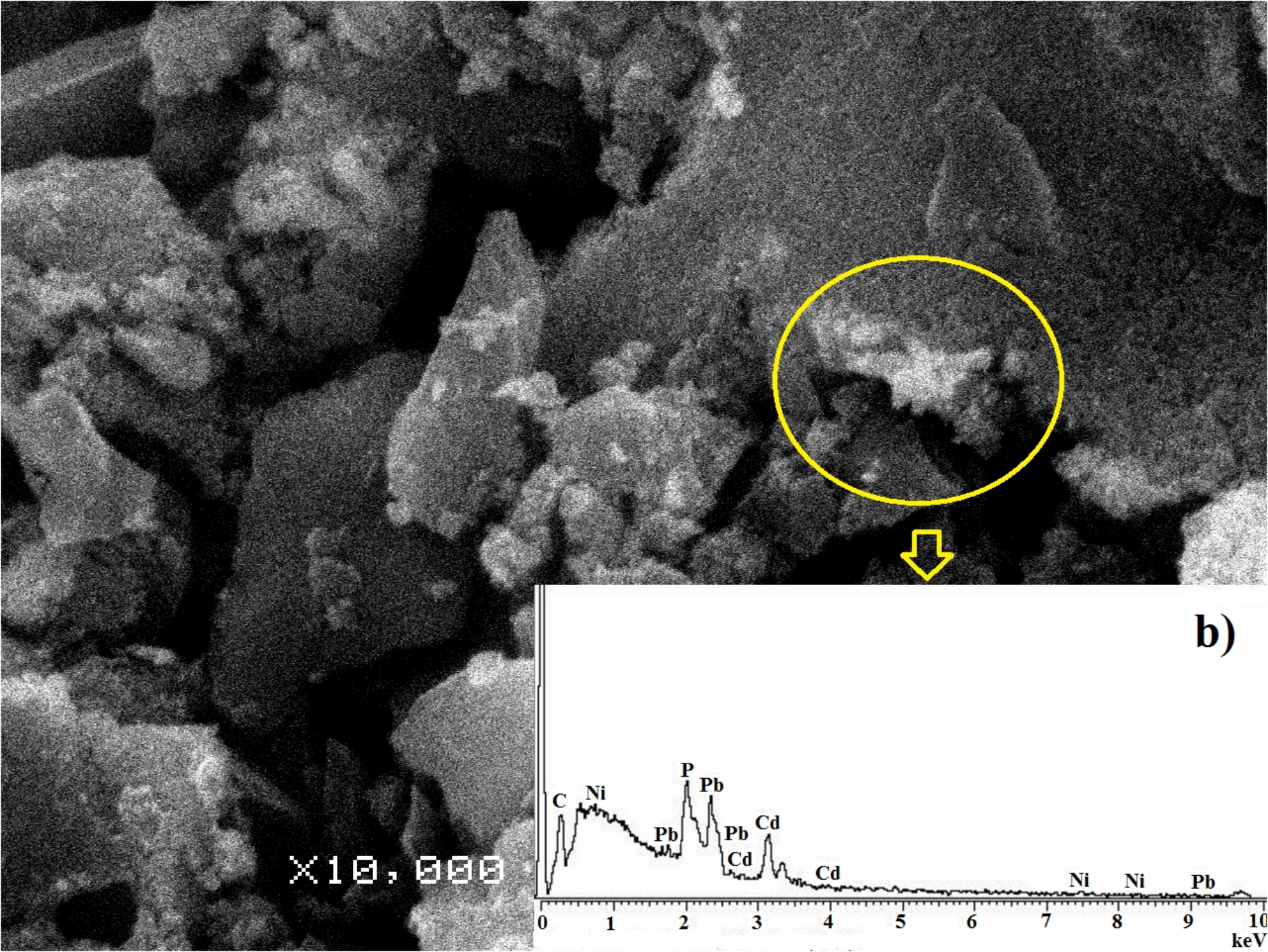
X10,000
b)
C
Ni
Pb
P
Pb
Pb
Cd
Cd
Cd
Ni
Ni
Pb
0
1
2
3
4
5
6
7
8
9
10
keV

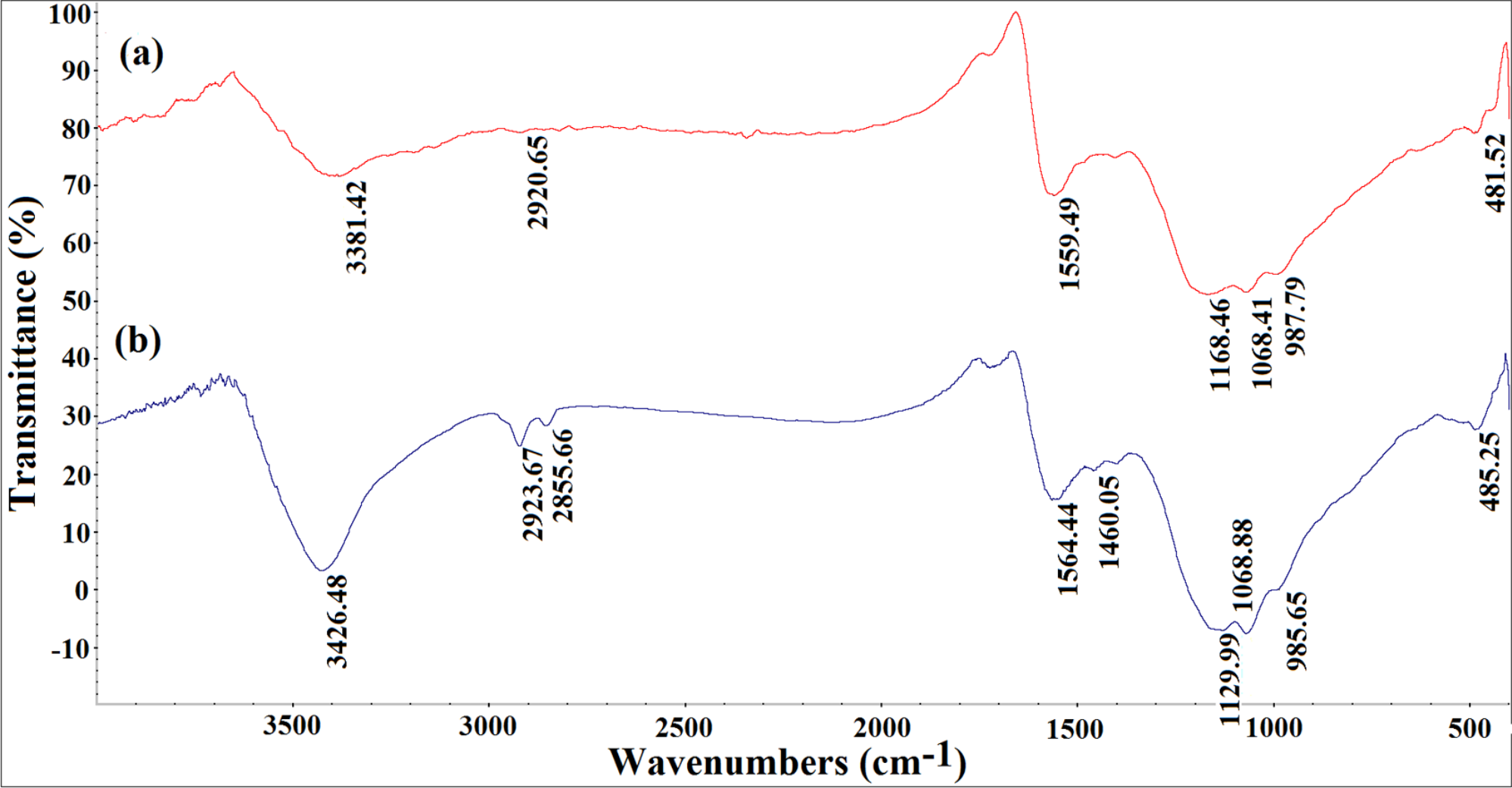
(a)
(b)
Transmittance (%)
Wavenumbers (cm-1)
100
90
80
70
60
50
40
30
20
10
0
-10
3500
3000
2500
2000
1500
1000
500
3381.42
2920.65
1559.49
1168.46
1068.41
987.79
481.52
3426.48
2923.67
2855.66
1564.44
1460.05
1129.99
1068.88
985.65
485.25

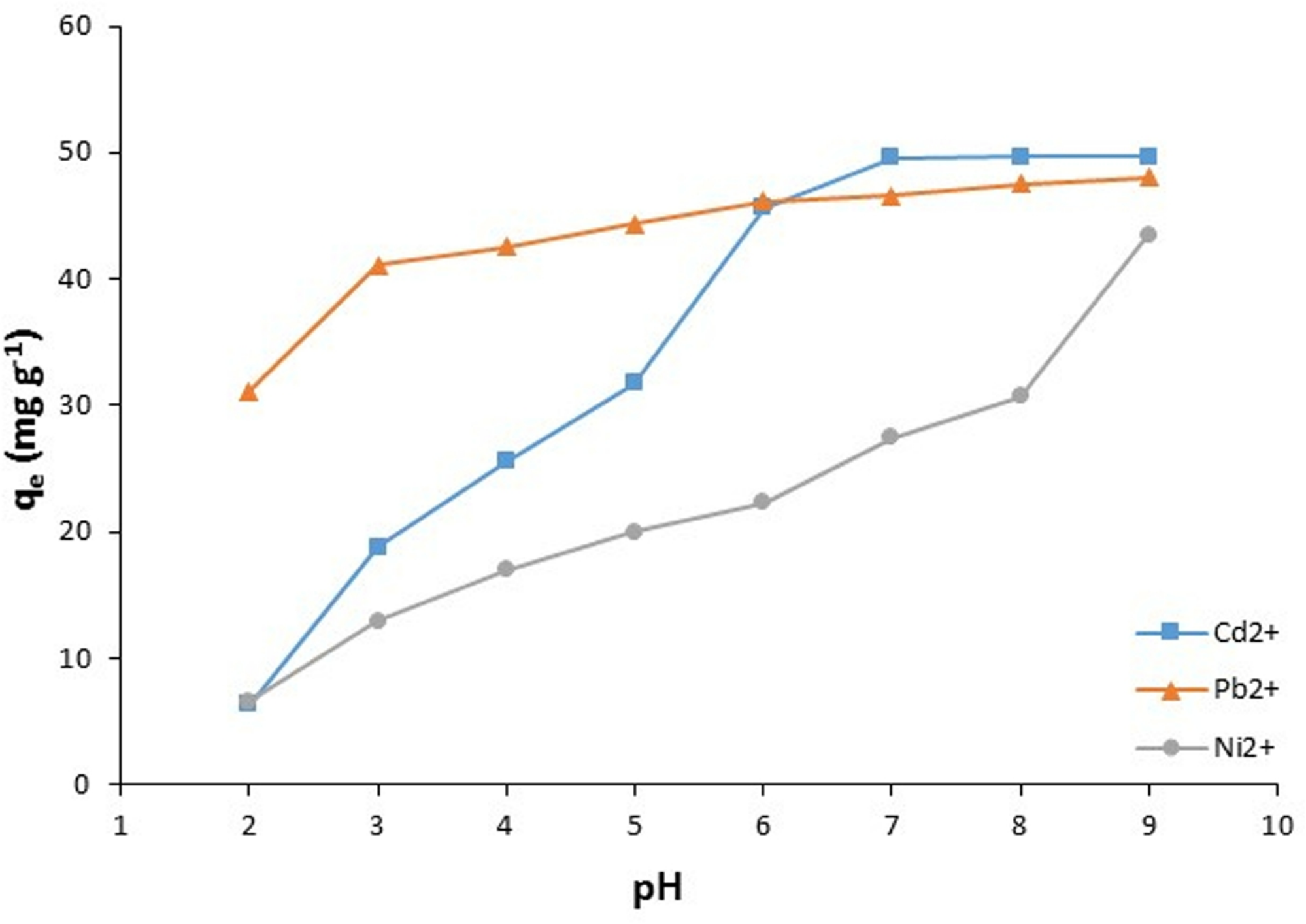
60
50
40
30
20
10
0
q_e (mg g^{-1})
1
2
3
4
5
6
7
8
9
10
pH
Cd2+
Pb2+
Ni2+

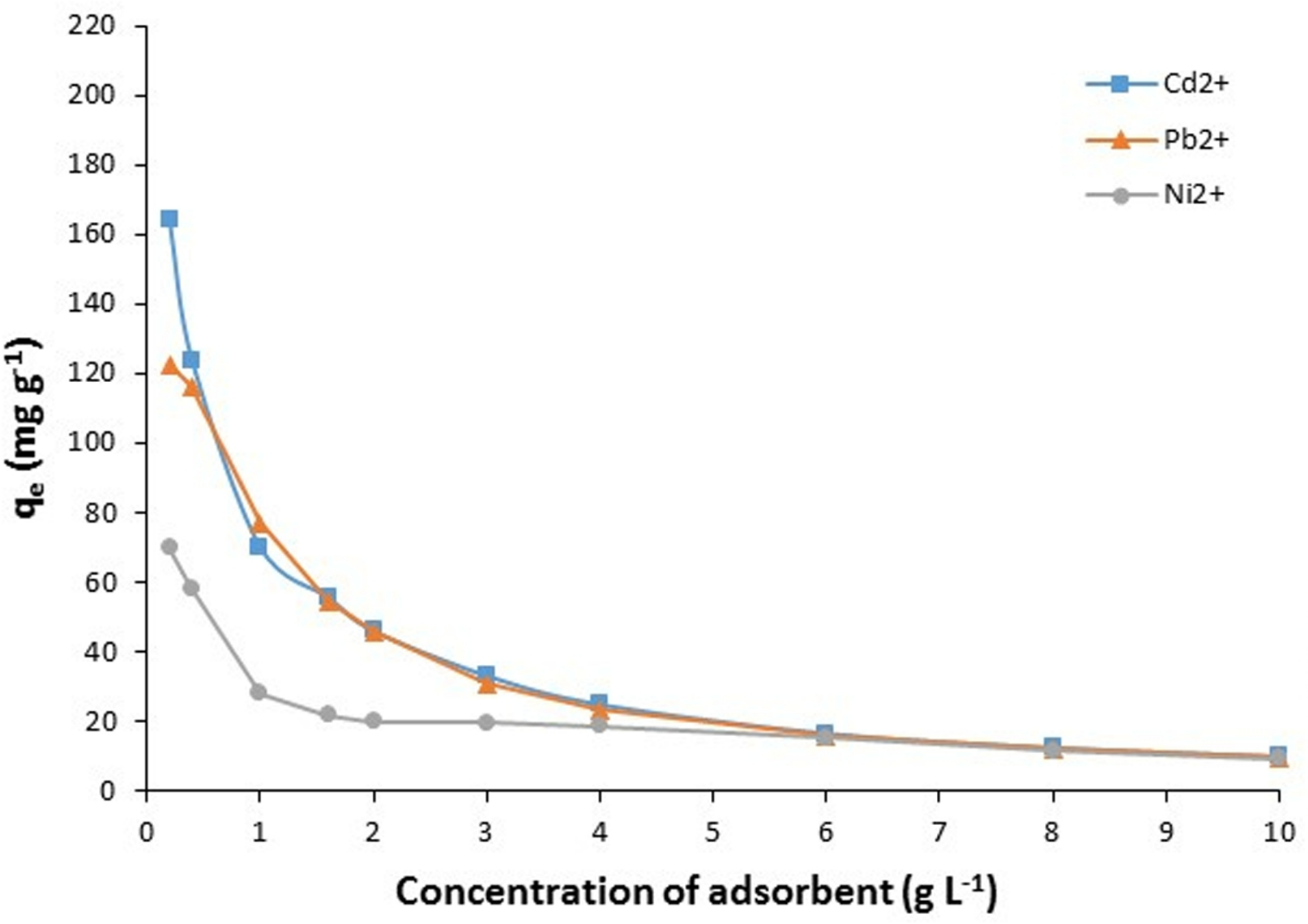
220
200
180
160
140
120
100
80
60
40
20
0
q_e (mg g^{-1})
0
1
2
3
4
5
6
7
8
9
10
Concentration of adsorbent (g L^{-1})
Cd2+
Pb2+
Ni2+

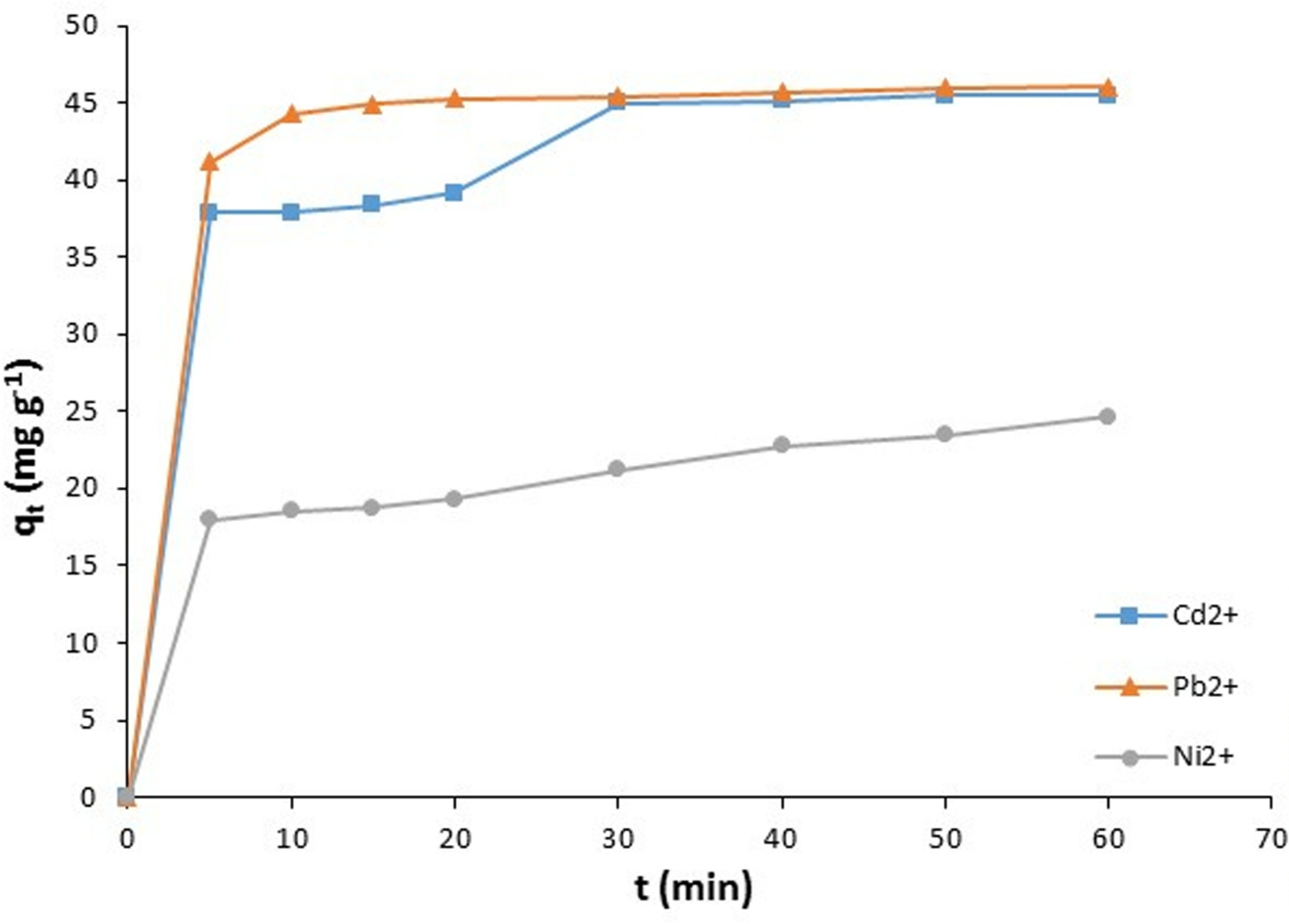
50
45
40
35
30
25
20
15
10
5
0
q_t (mg g^{-1})
0
10
20
30
40
50
60
70
t (min)
Cd2+
Pb2+
Ni2+

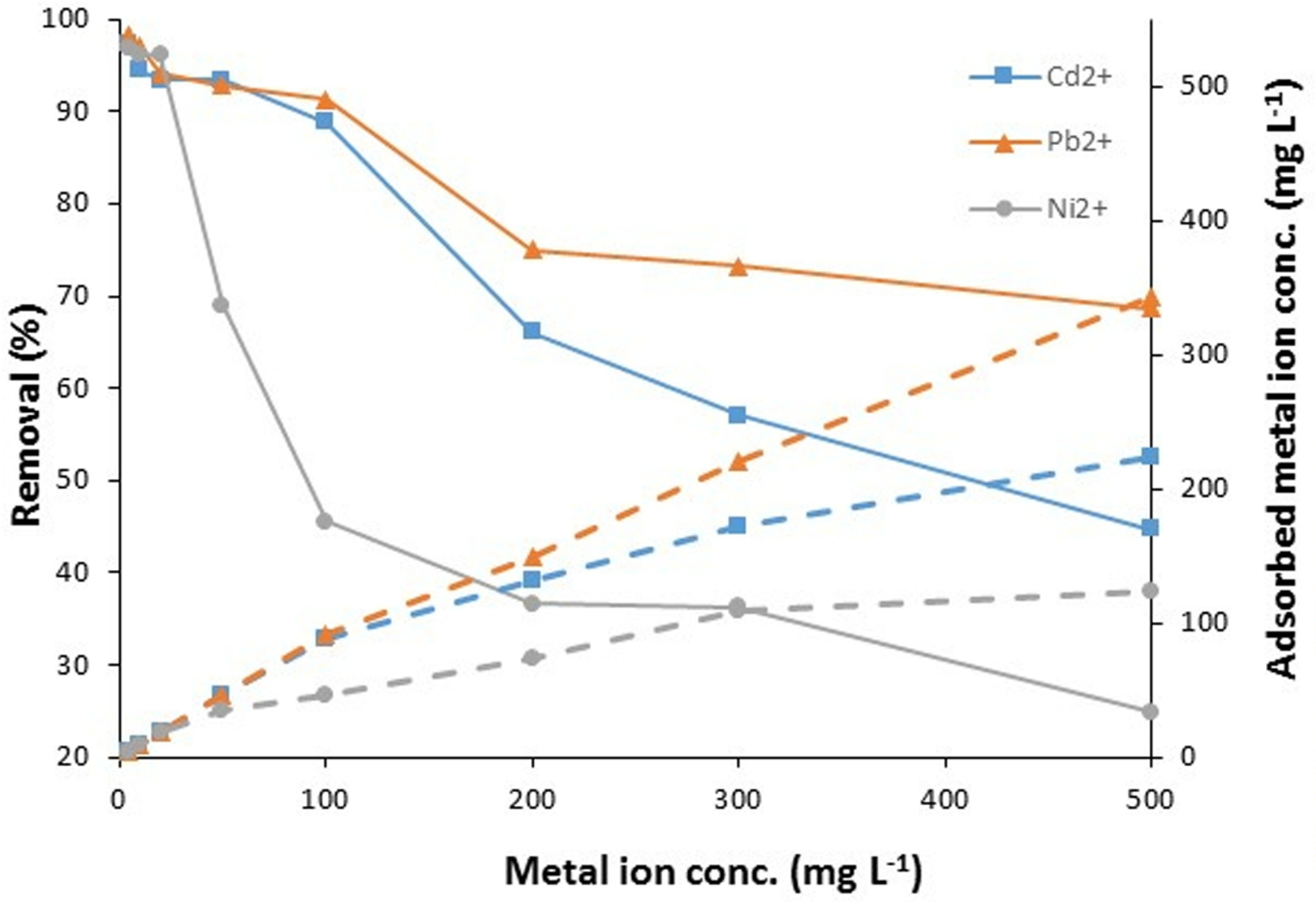
Removal (%)
Adsorbed metal ion conc. (mg L-1)
Metal ion conc. (mg L-1)
Cd2+
Pb2+
Ni2+
100
90
80
70
60
50
40
30
20
500
400
300
200
100
0
0
100
200
300
400
500

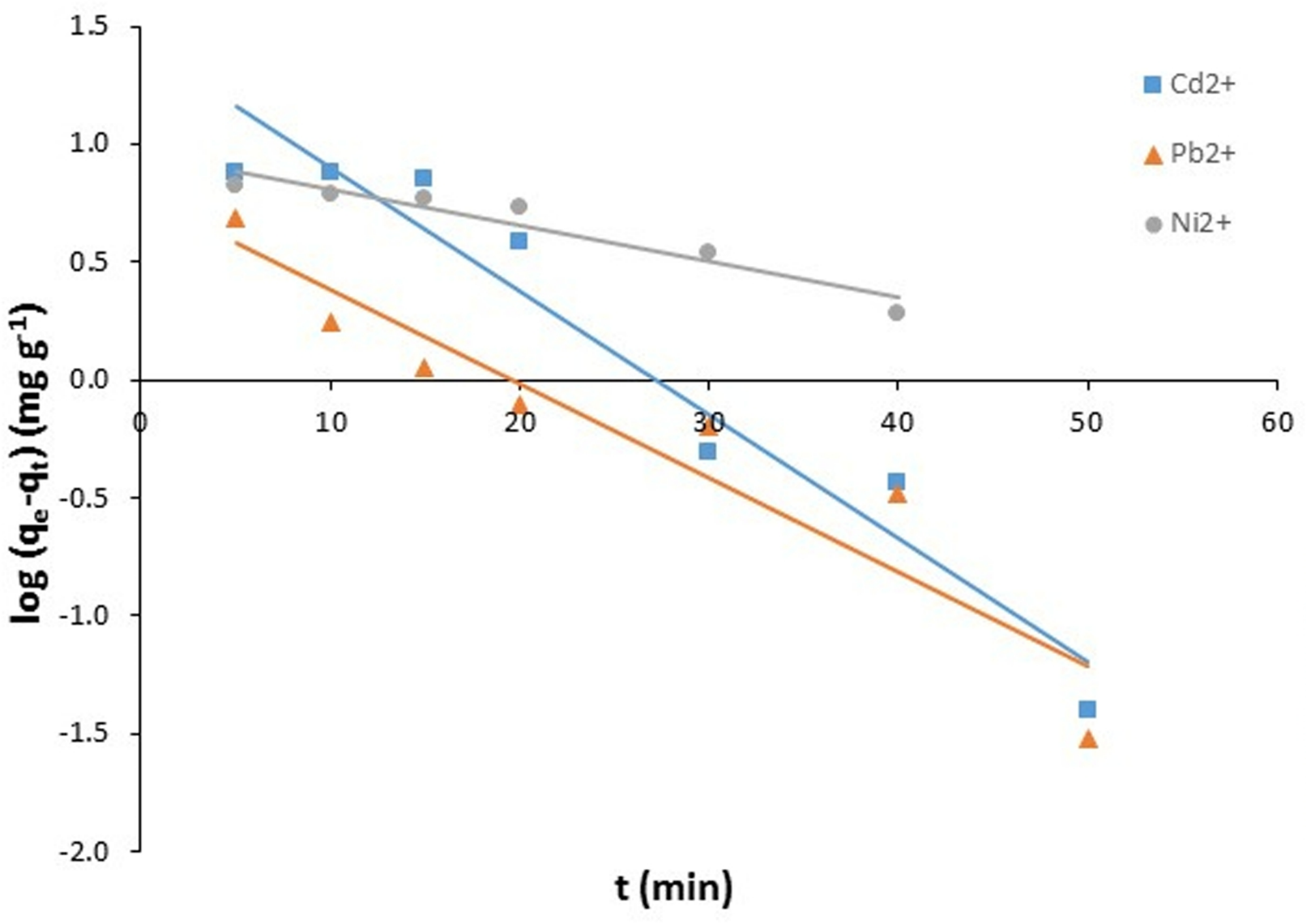
1.5
1.0
0.5
0.0
-0.5
-1.0
-1.5
-2.0
0
10
20
30
40
50
60
log (qe-qt) (mg g-1)
t (min)
Cd2+
Pb2+
Ni2+

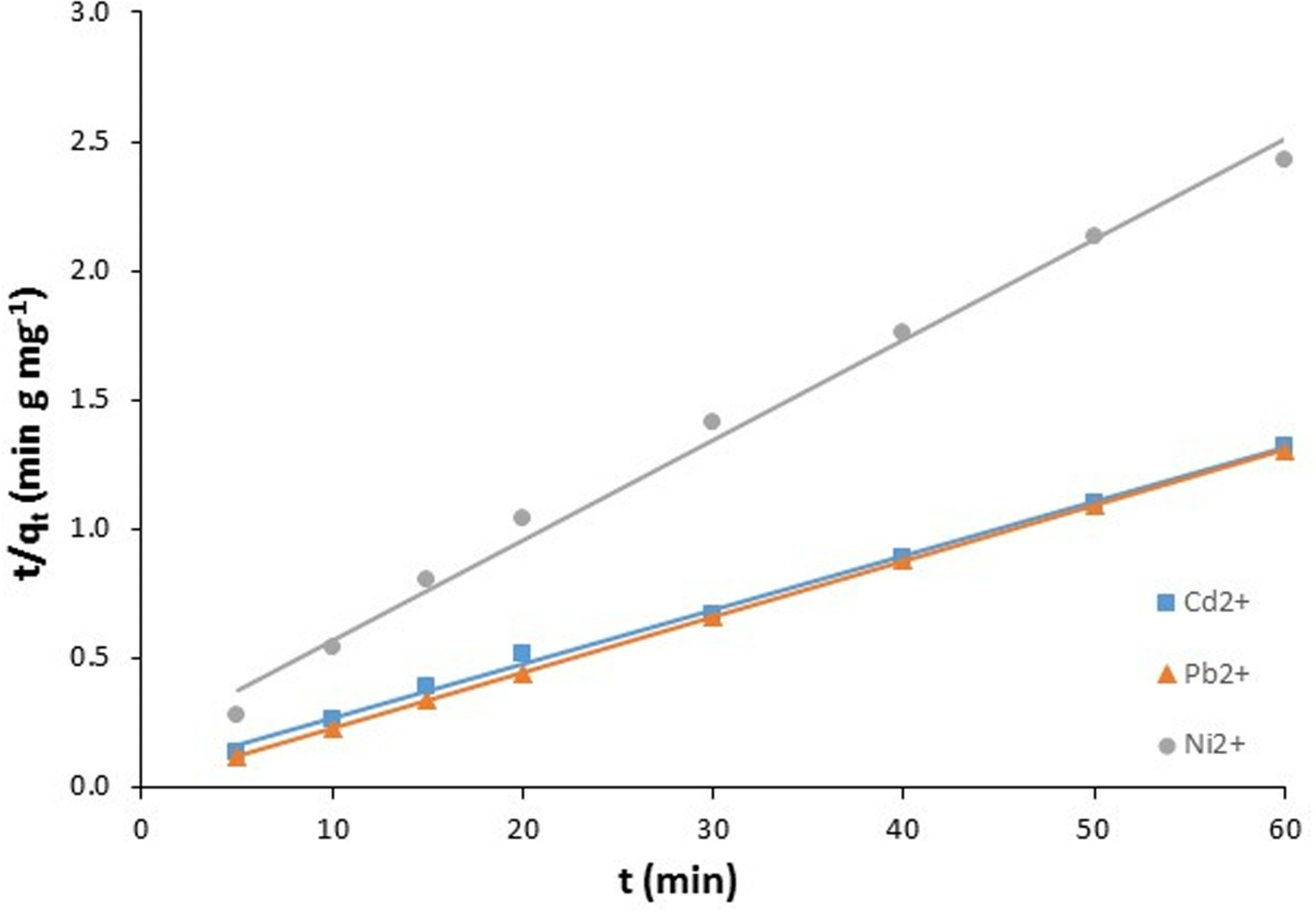
3.0
2.5
2.0
1.5
1.0
0.5
0.0
t/qt (min g mg-1)
0
10
20
30
40
50
60
t (min)
Cd2+
Pb2+
Ni2+

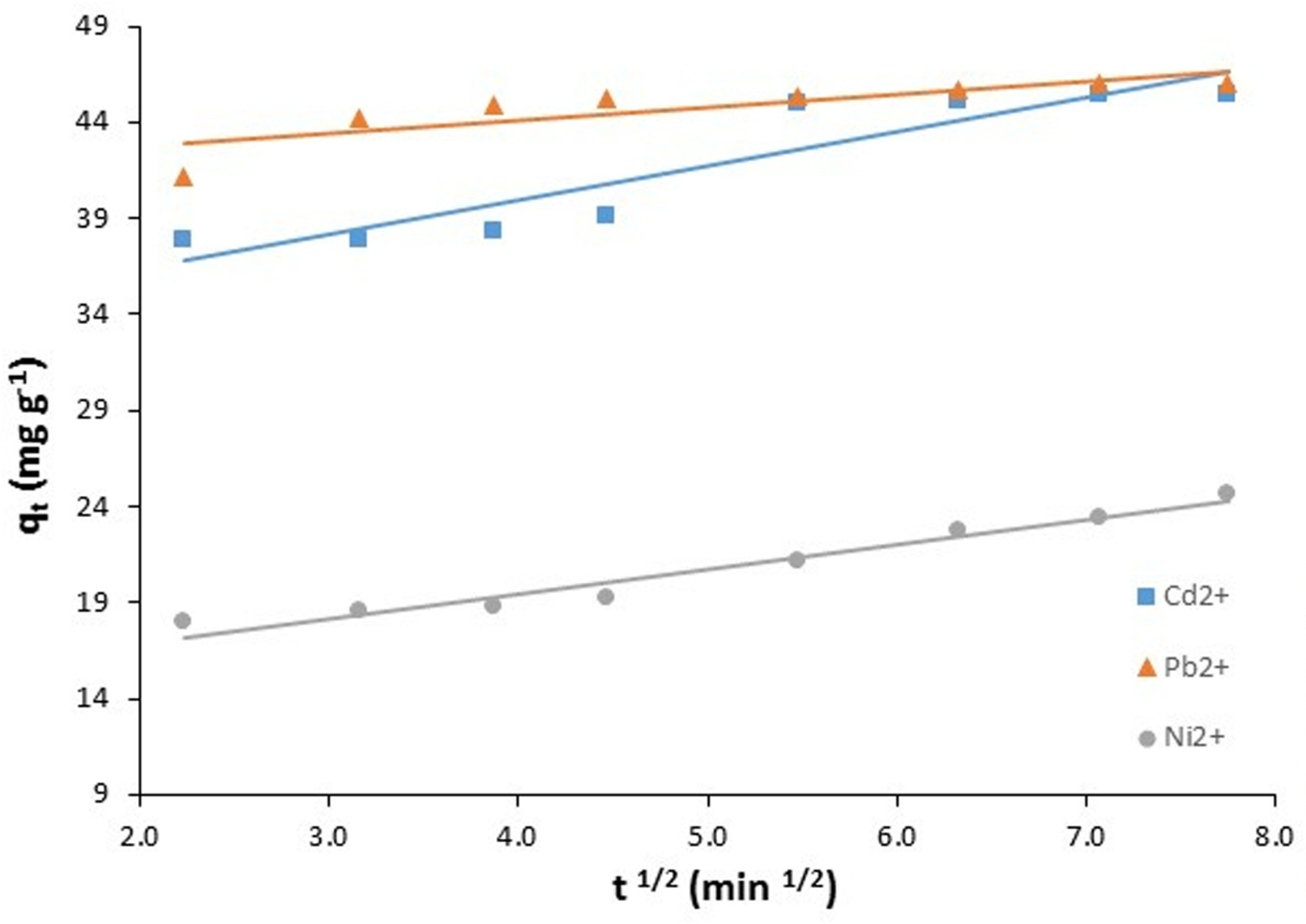
49
44
39
34
29
24
19
14
9
q_t (mg g^{-1})
2.0
3.0
4.0
5.0
6.0
7.0
8.0
$t^{1/2}$ (min $^{1/2}$)
Cd2+
Pb2+
Ni2+

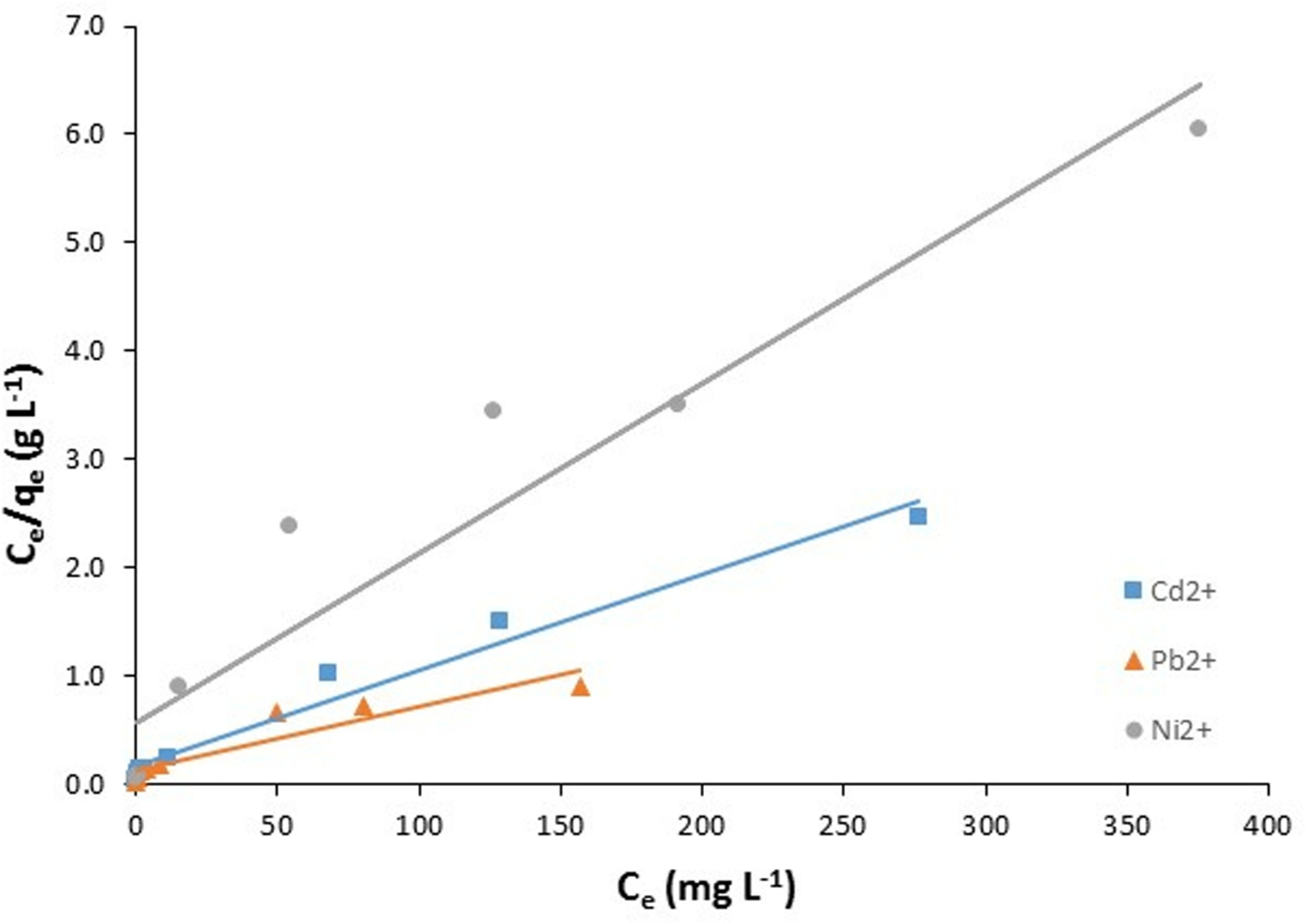
7.0
6.0
5.0
4.0
3.0
2.0
1.0
0.0
C_e/q_e (g L^{-1})
0
50
100
150
200
250
300
350
400
C_e (mg L^{-1})
Cd2+
Pb2+
Ni2+

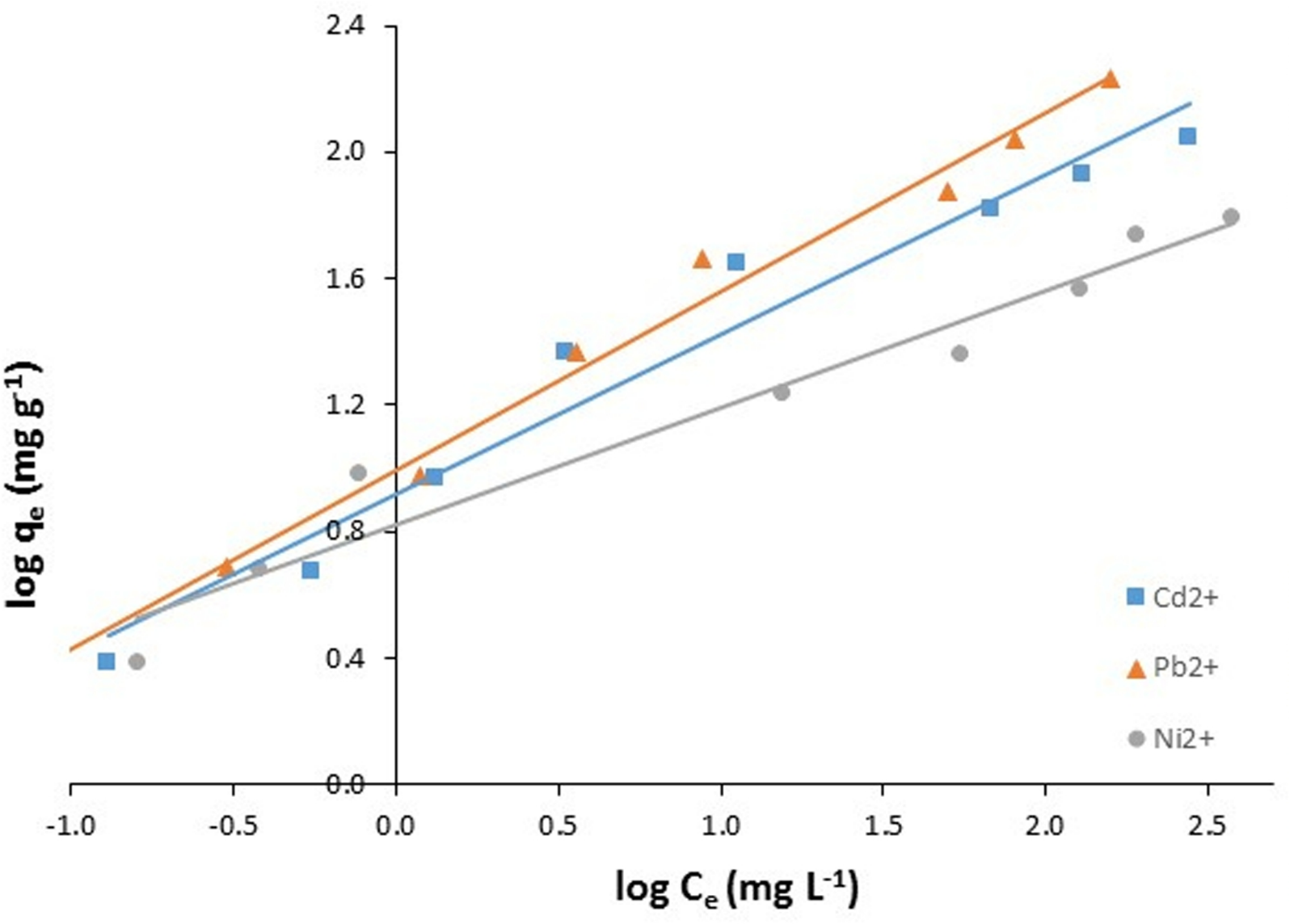
2.4
2.0
1.6
1.2
0.8
0.4
0.0
-1.0
-0.5
0.0
0.5
1.0
1.5
2.0
2.5
log qe (mg g-1)
log Ce (mg L-1)
Cd2+
Pb2+
Ni2+

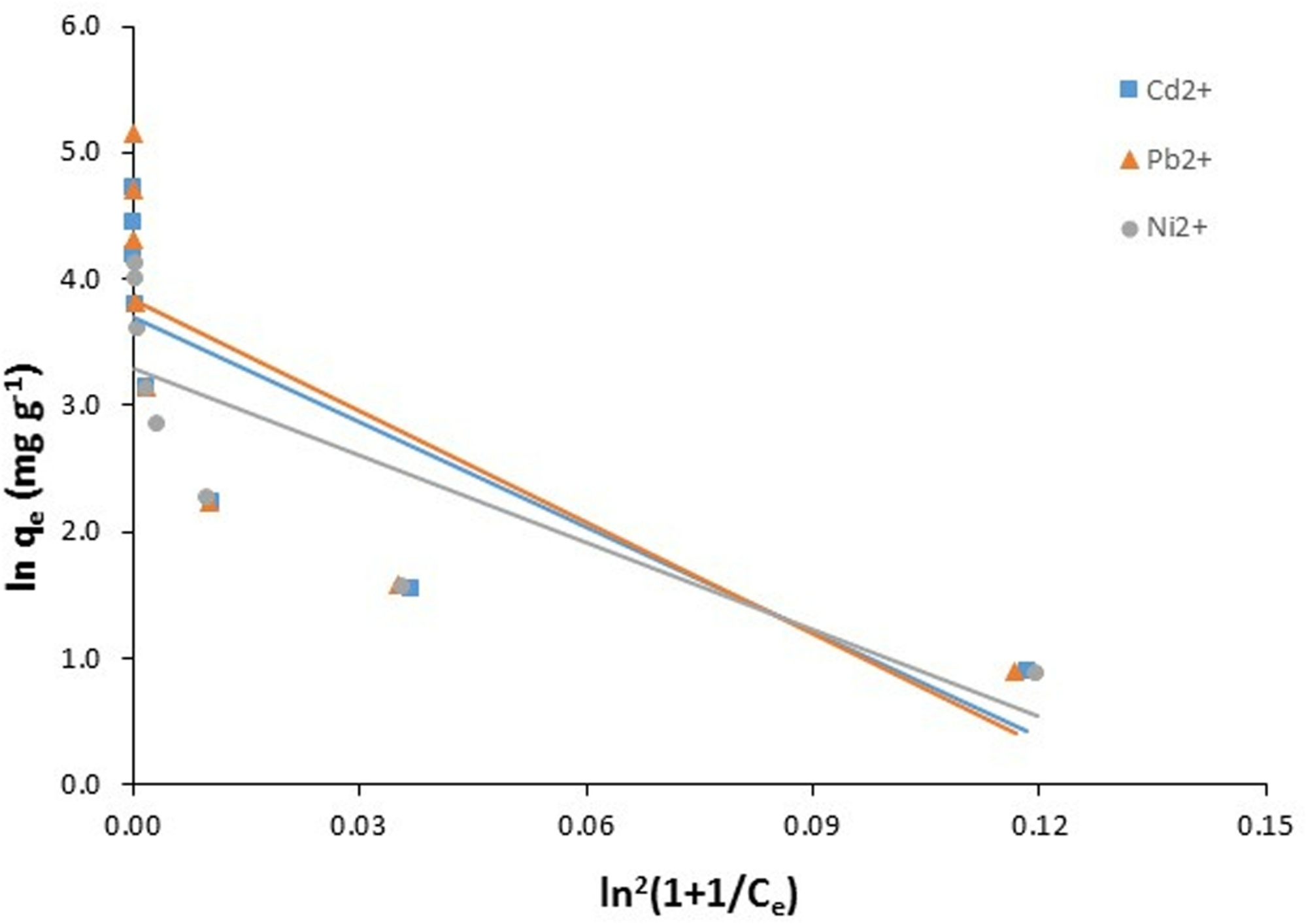
6.0
5.0
4.0
3.0
2.0
1.0
0.0
0.00
0.03
0.06
0.09
0.12
0.15
ln qe (mg g-1)
ln2(1+1/Ce)
Cd2+
Pb2+
Ni2+

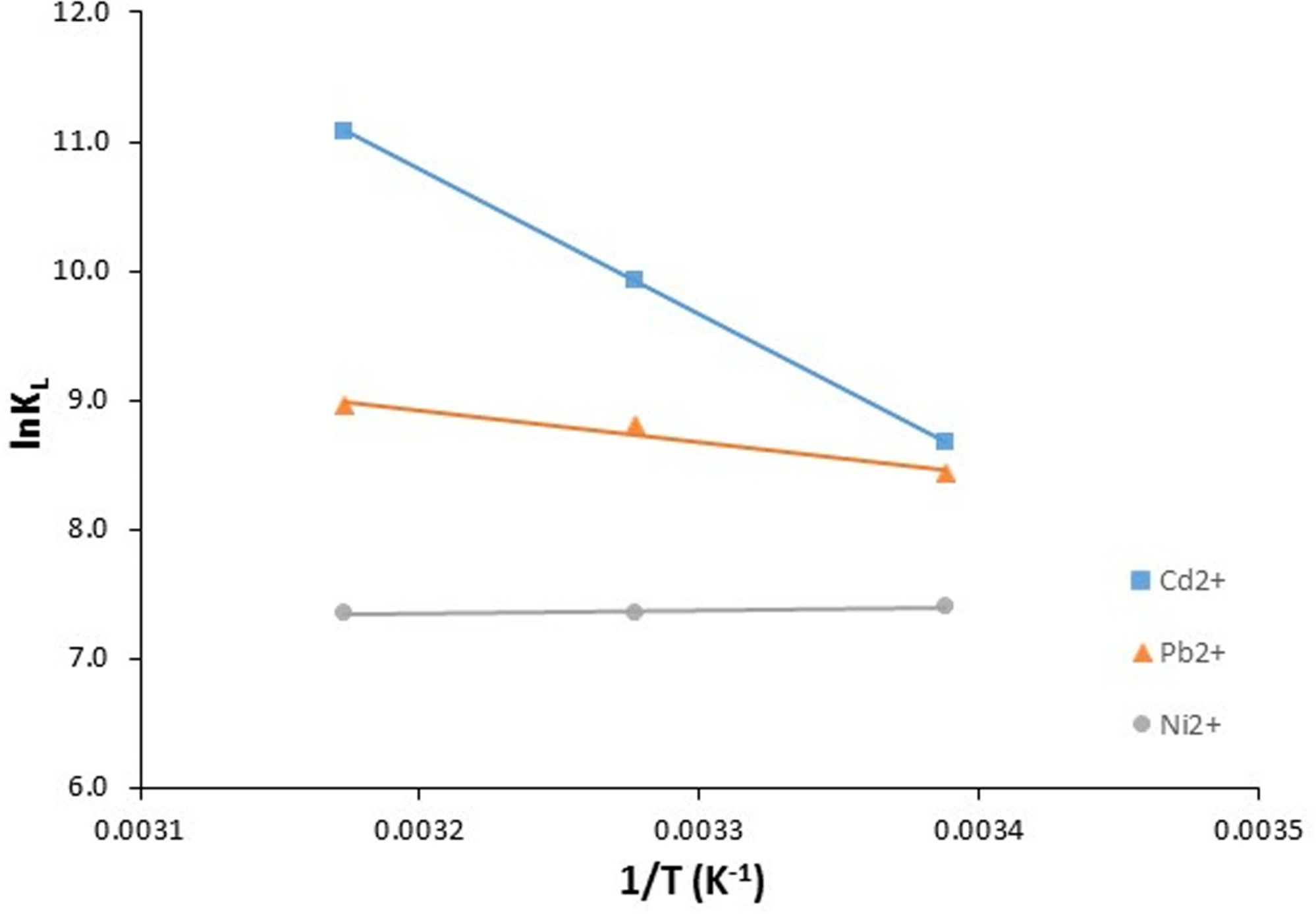
12.0
11.0
10.0
9.0
8.0
7.0
6.0
lnK_L
0.0031
0.0032
0.0033
0.0034
0.0035
1/T (K-1)
Cd2+
Pb2+
Ni2+

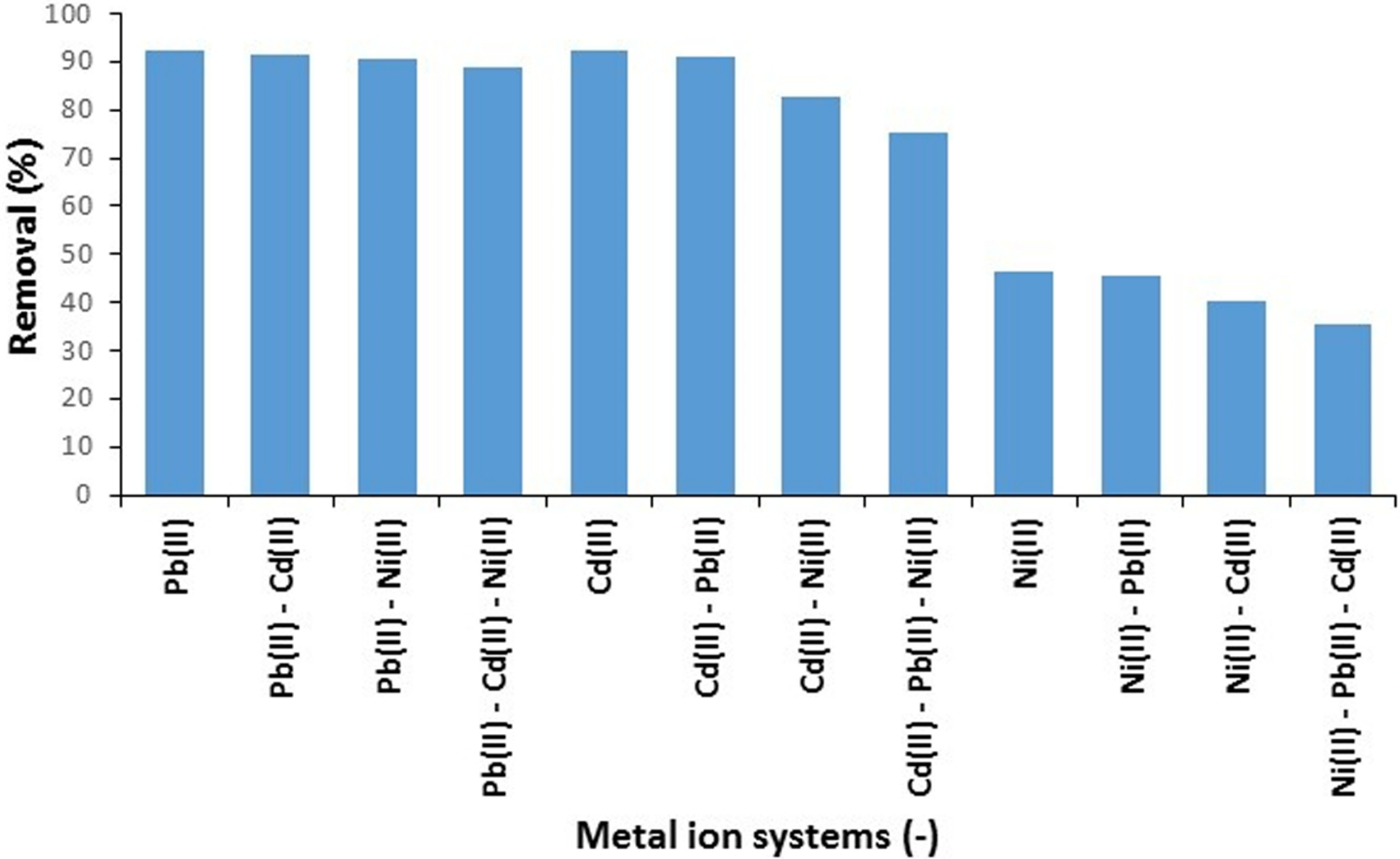
Removal (%)
100
90
80
70
60
50
40
30
20
10
0
Pb(II)
Pb(II) - Cd(II)
Pb(II) - Ni(II)
Pb(II) - Cd(II) - Ni(II)
Cd(II)
Cd(II) - Pb(II)
Cd(II) - Ni(II)
Cd(II) - Pb(II) - Ni(II)
Ni(II)
Ni(II) - Pb(II)
Ni(II) - Cd(II)
Ni(II) - Pb(II) - Cd(II)
Metal ion systems (-)

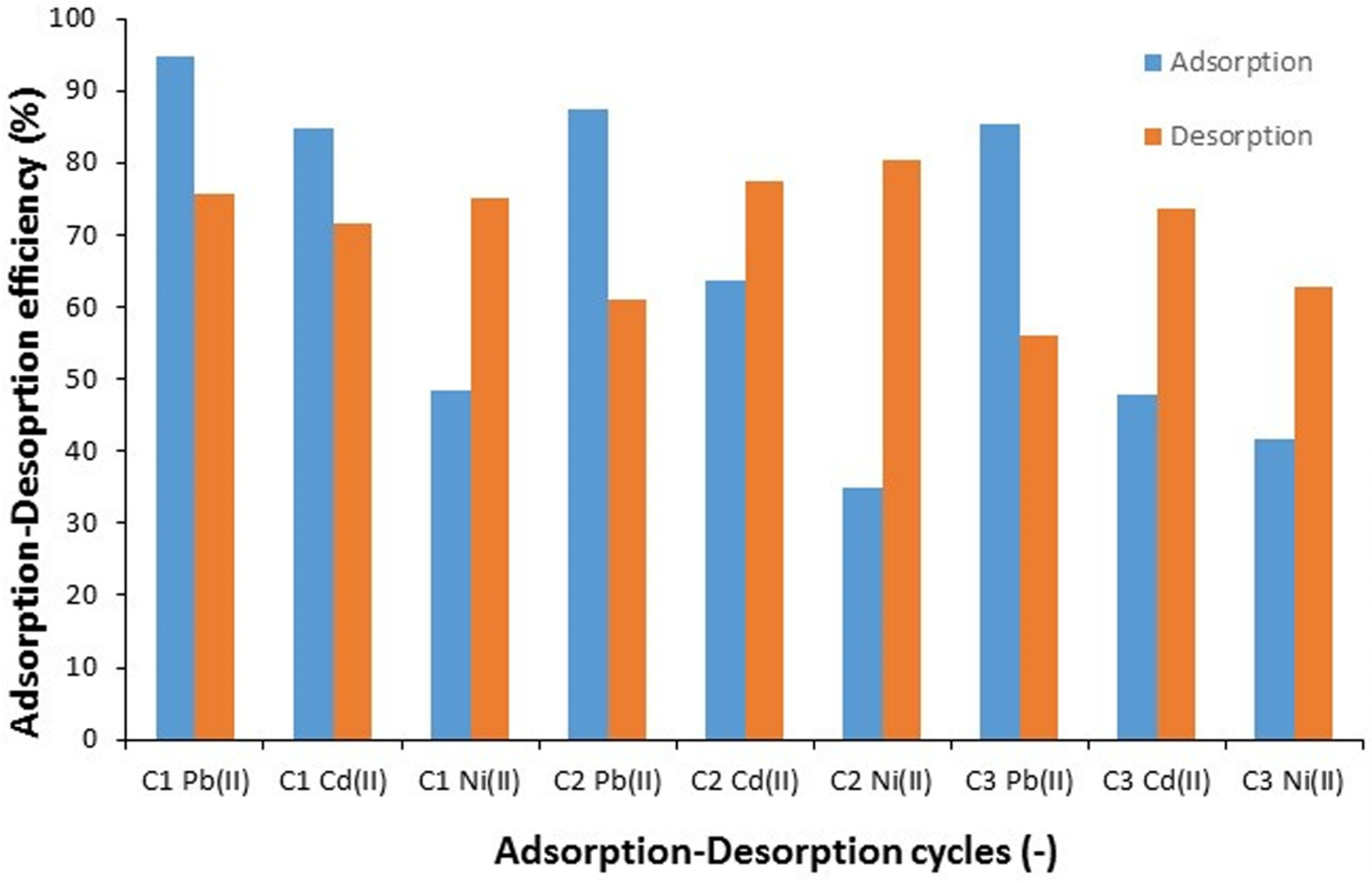
Adsorption
Desorption
Adsorption-Desoprtion efficiency (%)
100
90
80
70
60
50
40
30
20
10
0
C1 Pb(II)
C1 Cd(II)
C1 Ni(II)
C2 Pb(II)
C2 Cd(II)
C2 Ni(II)
C3 Pb(II)
C3 Cd(II)
C3 Ni(II)
Adsorption-Desorption cycles (-)

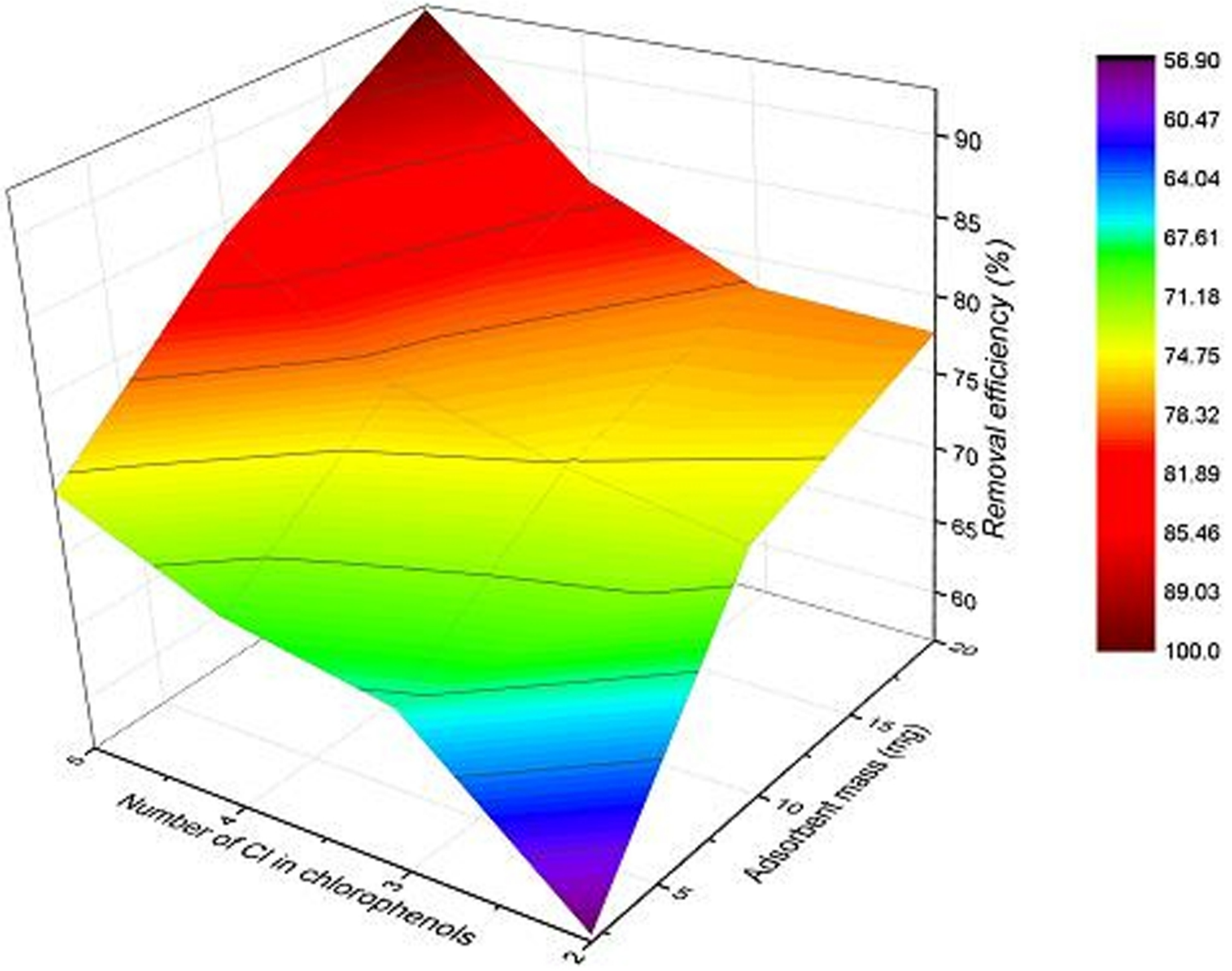
Removal efficiency (%)
90
85
80
75
70
65
60
Number of Cl in chlorophenols
5
4
3
2
Adsorbent mass (mg)
20
15
10
5
56.90
60.47
64.04
67.61
71.18
74.75
78.32
81.89
85.46
89.03
100.0

Plum stones

Pretreatment

Pretreated biomass

Thermochemical activation

Engineered activated carbon